Phytochemistry 164 (2019) xxx–xxx

Contents lists available at ScienceDirect

Phytochemistry

journal homepage: www.elsevier.com/locate/phytochem

NMR characterization and evaluation of antibacterial and antiobiofilm activity of organic extracts from stationary phase batch cultures of five marine microalgae (*Dunaliella* sp., *D. salina*, *Chaetoceros calcitrans*, *C. gracilis* and *Tisochrysis lutea*)

M[a] José Iglesias[a,*], Raquel Soengas[a], Ian Probert[b], Emilie Guilloud[b], Priscillia Gourvil[b], Mohamed Mehiri[c], Yuly López[d], Virginio Cepas[d], Ignacio Gutiérrez-del-Río[e], Saúl Redondo-Blanco[e], Claudio J. Villar[e], Felipe Lombó[e], Sara Soto[d], Fernando López Ortiz[a,**]

[a] Área de Química Orgánica, Research Centre CIAIMBITAL, Universidad de Almería, Carretera de Sacramento s/n, Almería, 04120, Spain
[b] Roscoff Culture Collection, FR2424 Station Biologique de Roscoff (Sorbonne Université / CNRS), 29680, Roscoff, France
[c] Institut de Chimie de Nice, UMR CNRS 7272, Université Nice Sofia Antopolis, 06103, Nice, France
[d] Barcelona Institute for Global Health (ISGlobal)-Hospital Clinic-Universitat de Barcelona, Carrer Rosselló 132, 08036, Barcelona, Spain
[e] Research Group BIONUC, Departamento de Biología Funcional, Área de Microbiología, University of Oviedo, Oviedo, Principality of Asturias, Spain. IUOPA (Instituto Universitario de Oncología del Principado de Asturias), ISPA (Instituto de Investigación Sanitaria del Principado de Asturias), Spain

ARTICLE INFO

Keywords:
Dunaliella
Chaetoceros
Tisochrysis
NMR
Metabolite identification
Antibacterial
Antibiofilm

ABSTRACT

The chemical composition of five marine microalgae (*Dunaliella* sp., *Dunaliella salina*, *Chaetoceros calcitrans*, *Chaetoceros gracilis* and *Tisochrysis lutea*) was investigated through nuclear magnetic resonance (NMR) spectroscopic study of the soluble material obtained by sequential extraction with hexane, ethyl acetate (AcOEt) and methanol of biomass from stationary phase cultures. Hexane extracted the major lipids present in the microalgae during the stationary phase of growth, which correspond to storage lipids. Triacylglycerols (TGs) were the only storage lipids produced by *Dunaliella* and *Chaetoceros*. In contrast, *T. lutea* predominantly stored polyunsaturated long-chain alkenones, with sterols also detected as minor components of the hexane extract. The molecular structure of brassicasterol was determined in *T. lutea* and the presence of squalene in this sample was also unequivocally detected. Monogalactosyldiacylglycerols (MGDGs) and pigments were concentrated in the AcOEt extracts. *C. calcitrans* and *D. salina* constituted an exception due to the high amount of TGs and glycerol produced, respectively, by these two strains. Chlorophylls *a and b* and β-carotene were the major pigments synthesized by *Dunaliella* and chlorophyll *a* and fucoxanthin were the only pigments detected in *Chaetoceros* and *T. lutea*. Information concerning the acyl chains present in TGs and MGDGs as well as the positional distribution of acyl chains on the glycerol moiety was obtained by NMR analysis of hexane and AcOEt extracts, with results consistent with those expected for the genera studied. Fatty acid composition of TGs in the two *Dunaliella* strains was different, with polyunsaturated acyl chains almost absent in the storage lipids produced by *D. salina*. Except in *C. calcitrans*, the polar nature of soluble compounds was inferred through the relative extraction yield using methanol as the extraction solvent. Glycerol was the major component of this fraction for the *Dunaliella* strains. In *T. lutea* 1,4/2,5-cyclohexanetetrol (CHT) and dimethylsulfoniopropionate (DMSP) preponderated. CHT was also the major polyol present in the *Chaetoceros* strains in which DMSP was not detected, but prominent signals of 2,3-dihydroxypropane-1-sulfonate (DHSP) were observed in the 1H NMR spectra of methanolic extracts. The presence of DHSP confirms the production of this metabolite by diatoms. In addition, several other minor compounds (digalactosyldiacyglycerols (DGDGs), sulphoquinovosyldiacylglycerols (SQDGs), amino acids, carbohydrates, *scyllo*-inositol, mannitol, lactic acid and homarine) were also identified in the methanolic extracts. The antibacterial and antibiofilm activities of the extracts were tested. The AcOEt extract from *C. gracilis* showed a moderate antibiofilm activity.

* Corresponding author. Área de Química Orgánica, Universidad de Almería. Carretera de Sacramento s/n, 04120 Almería, Spain.
** Corresponding author. Área de Química Orgánica, Universidad de Almería. Carretera de Sacramento s/n, 04120 Almería, Spain.
E-mail addresses: mjigle@ual.es (M.J. Iglesias), flortiz@ual.es (F.L. Ortiz).

https://doi.org/10.1016/j.phytochem.2019.05.001
Received 9 January 2019; Received in revised form 11 April 2019; Accepted 6 May 2019

1. Introduction

Microalgae are photosynthetic organisms that display high levels of bio- and chemo-diversity due to the wide range of habitats in which they live and the ability to survive in competitive environments. The estimated total number of microalgal species ranges from 200,000 to 800,000, but only about 35,000 have been formally described and the number that have been comprehensively examined from the structural-chemical point of view is extremely lower (Guiry, 2012; Mobin and Alam, 2017). Characterization of the chemical composition of microalgae is important in order to obtain taxonomic information (Lang et al., 2011) and also to promote rational use of this important natural resource. The unique composition (notably of lipids) of microalgae means they have enormous potential for applications in important biotechnological fields such as biofuel production, human nutrition, aquaculture and the discovery of novel active compounds (Wikfors and Ohno, 2001; Guiry, 2012; Bhattacharjee, 2016; Matos, 2017; Chia et al., 2018). Furthermore, the rapid growth rate potentially facilitates large-scale biomass production with manipulation of cultivation conditions being a tool to increase the production of relevant metabolites. Microalgae can thus be considered one of the most promising sources for new products and applications, but their commercial exploitation is limited mainly due the time and cost required to develop new products, as well as issues of market demand and consumer acceptation.

Marine organisms are the subject of widespread interest in the field of drug discovery, being widely considered as a promising source of compounds with unique chemical structures and biological activities in comparison with terrestrial metabolites (Blunt et al., 2015; Jaspars et al., 2016; Romano et al., 2017). To date, marine natural products have mainly been applied in anticancer chemotherapy. In contrast, the investigation of antibacterial activity of marine extracts is less developed (Mayer et al., 2013; Shannon and Abu-Ghannam, 2016). However, there is a pressing need to develop new antibiotics due to the dramatic increase of multi-resistant bacterial strains as a result of the overuse of existing antibiotics. Furthermore, the formation of bacterial biofilms on medical devices and implants constitutes a major problem being associated, in many cases, with persistent infections. Lipids are well-known for antibacterial activity (Thormar, 2011) and the high lipid content and unique lipid composition of microalgae make them strong candidates as a source for compounds with antibacterial and antibiofilm activity. In contrast to higher plants, many algae, in particular marine species, are able to synthetise very long chain polyunsaturated fatty acids (PUFAs). The antibacterial properties of microalgal fatty acids against a range of Gram-positive and Gram-negative bacteria that include the multidrug-resistant *Staphyloccoccus aureus* have been reported (Ohta et al., 1995; Zheng et al., 2005; Desbois and Mearns-Spragg, 2009; Ruffell et al., 2016). On the other hand, the production of anti-quorom sensing compounds for the cyanobacteria *Anabaena* sp. and *Lyngbya majuscula* has been reported (Romero et al., 2008; Dobretsov et al., 2010). Moreover, an efficient inhibition on biofilm formation by clinical significant bacteria has been found for extracts of *Spirulina platensis* (LewisOscar et al., 2017) and for two species of the *Leptocylindrus* genus (Lauritano et al., 2016).

Solvent extraction is the first step in metabolite isolation (Sarker et al., 2006). The metabolome comprises numerous compounds that strongly vary in chemical nature, solubility and concentration. Metabolite composition is inevitably biased by the extraction procedure and a single solvent is not sufficient for the analysis of all metabolites. Sequential extraction with solvents of increasing polarity allows a preliminary separation of the metabolites present in the original material, which facilitates the characterization of the extracts and downstream isolation of given compounds. Once soluble material is obtained, efficient analytical methods are required for comparative and screening studies. In this context, NMR spectroscopy is a powerful tool in metabolic studies (Fan and Lane, 2016; Deborde et al., 2017). NMR spectroscopy is a rapid, non-destructive, high-throughput method for identifying and quantifying the most abundant metabolites present in biological material. The suitability of NMR techniques for algae analysis was underlined for more than two decades (Pollesello et al. 1992). In contrast to convectional chromatographic methods that require further fractionation and derivatization for full lipid characterization, the information contained in a single NMR spectrum covers a wide range of compounds. Nonetheless, reports on the analysis of microalgae lipid fraction by NMR are limited (Beal et al., 2010; Nuzzo et al., 2013; Kumar et al., 2014; Sarpal et al., 2015, 2016a, 2016b, 2016c). Similarly, metabolomic studies of algal species are also scarce (Kim et al., 2006; Gupta et al., 2013; Akhter et al., 2016; Azizan et al., 2018; Chauton and Størseth, 2018; Réveillon et al., 2018). The high chemodiversity of these organisms makes metabolite identification a complex and challenging issue. In a very recent work, Azizan et al. (2018) have tried to correlate the 1H metabolic profiling of *Chaetoceros calcitrans* soluble material obtained using different solvents with antioxidant activity. They reported the identification of 29 metabolites. However, some structural assignments are not adequately supported by the experimental data provided, which gives rise to inconsistencies in chemical composition. Moreover, the attempts to make a semiquantification based on variables deduced from the assignment of signals with contribution from several compounds to a specific metabolite impair reliability to the conclusions obtained.

In the present study, biomass from stationary phase batch cultures of five marine microalgae species, *Dunaliella* sp. and *Dunaliella salina* (Chlorophyta), *Chaetoceros calcitrans* and *Chaetoceros gracilis* (Bacillariophyta) and *Tisochrysis lutea* (Haptophyta), was sequentially extracted using hexane, ethyl acetate and methanol as solvents. The microalgae studied here constitute a selection of species with existing industrial interest. *Dunaliella* is cultivated for the production of carotene and glycerol, with β-carotene obtained from *D. salina* being the first valuable product commercially produced from a microalgae. *Chaetoceros* and *Tisochrysis lutea* are used extensively as food source in aquaculture. Lipid composition and, in particular, the content in the polyunsaturated fatty acids (PUFAs) arachidonic acid (ARA, C20:4 ω-6), docosahexaenoic acid (DHA, C22:6 ω-3) and eicosapentaenoic acid (EPA, C20:5 ω-3), are important factors for the nutritional evaluation of an algae species used as food for cultivated marine organisms (Volkman et al., 1989; Wikfors and Ohno, 2001; Da Costa et al., 2016). The chemical composition of extracts from these microalgal species was analyzed by means of 1H and 13C NMR spectroscopy. Metabolite identification was carried out through the acquisition of 2D NMR experiments and by comparison with information in the literature. This analysis provides wide valuable information concerning the chemical constituents of the selected strains. A total of 34 metabolites of diverse nature were identified that allowed differentiation at the genus and even species level. The antibiotic activity and biofilm inhibition ability of the extracts were also tested.

2. Results and discussion

2.1. Compositional study

The distribution of the soluble material between extracts (Fig. 1) suggests that relatively polar compounds predominated except for *C. calcitrans* for which the relative amount of compounds extracted with hexane was the highest.

NMR analyses showed that extract composition was determined by the characteristics of the solvent. For each solvent the information contained in a spectrum covers a wide range of compounds without need of further separation and/or derivatization. This implies a difficulty in the identification of secondary metabolites because their signals can be masked by the signals due to the major compounds present in the complex mixture. Nevertheless, identification of several minor components was possible through of the combination of 1D and 2D NMR experiments. The metabolites identified in the five microalgae

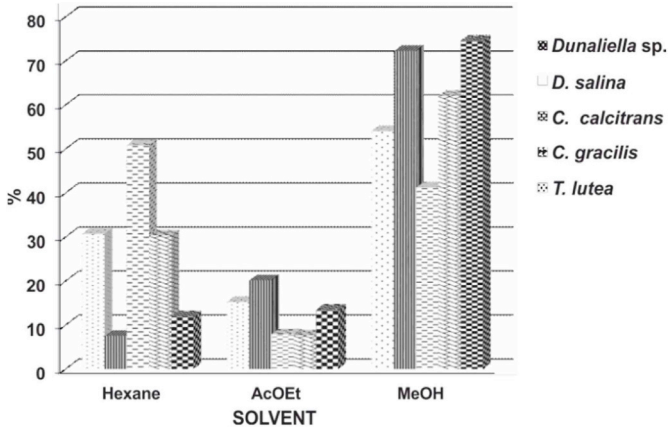

Fig. 1. Distribution of the soluble material (percentage of to the total soluble material recovered, dry basis).

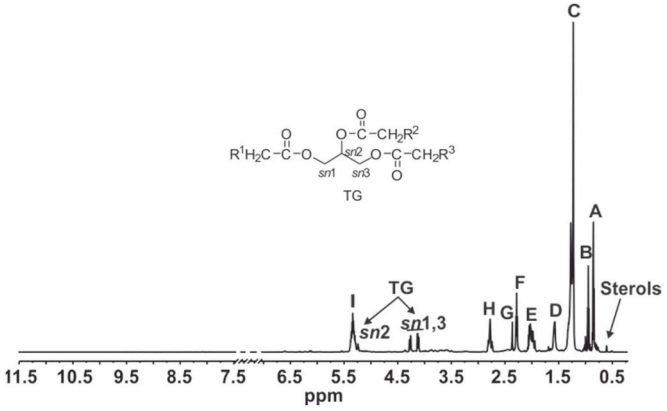

Fig. 2. 1H NMR spectrum of the hexane extract from *Dunaliella* sp. measured in $CDCl_3$. A: CH_3 in saturated acyl chains (SAFAs) and ω-9, ω-6 unsaturated acyl chains (UFAs). B: CH_3 in ω-3 PUFAs. C: $-(CH_2)_n-$. D: CH_2 β to C=O, except to Δ^4 acyl chains. E: Allylic CH_2, except CH_2 in β to C=O of Δ^4 acyl chains. F: CH_2 α to C=O, except Δ^4 acyl chains. G: CH_2 α and β to C=O in Δ^4 acyl chains. H: Bisallylic CH_2. I: Olefinic.

strains studied are summarized in Table 1 and their chemical structures and 1H and 13C NMR assignments are given in the Supplementary Material (Fig. S1 and Table S1, respectively).

2.1.1. Non- and semi-polar metabolites

Storage lipids accumulated by microalgae during the stationary phase were the major components of the hexane extracts. Triacylglycerols (TGs) were the only storage lipids present in the *Dunaliella* and *Chaetoceros* strains (Fig. 2, S2 and S3, Supplementary Material). The δ 5.3–3.0 ppm region of the 1H NMR spectra for these extracts showed the signals due to the glycerol backbone in TGs at δ 4.29 and 4.15 ppm for the *sn*1 and *sn*3 protons, respectively, and at δ 5.26 ppm for the *sn*2 proton (Fig. 2). The characteristic signals of acyl chains of fatty acids attached to the glycerol backbone resonated in the δ 3.00–0.50 ppm region (signals A-I in Fig. 2). Chemical shift of protons at the α-position to the carbonyl group, signals F and G centered at δ 2.31 and 2.39 ppm respectively, indicated that the acyl chains were esterified (Satyarthi et al., 2009; Nieva-Echevarría et al., 2014). This feature was also confirmed in the 13C NMR and HMBC spectra that

Table 1
Summary of metabolites identified by NMR spectroscopy in the extracts from the five marine microalgae strains analyzed.

	Chlorophyta		Bacillariophyta		Haptophyta
	Dunaliella		*Chaetoceros*		*T. lutea*
	sp.	*salina*	*calcitrans*	*gracilis*	
Storage lipids	TG	TG	TG	TG	PULCA TG (minor)
Membrane lipids	MGDG	MGDG	MGDG	MGDG	MGDG
	DGDG	DGDG	DGDG	DGDG	DGDG
	SQDG	SQDG	SQDG	SQDG	SQDG
Acyl chains	SAFA	SAFA	SAFA[a]	SAFA[a]	SAFA
	OL	OL	MUFA[b]	MUFA[b]	OL
	HDTA	HDTA	EPA	EPA	LO
	LO	LO	ARA	ARA	ALA
	ALA	ALA	C16:3 ϖ-4	C16:3 ϖ-4	SDA DHA
Pigments	Pheo a (a')	Pheo a (a')	Pheo a (a')	Pheo a (a')	Pheo a (a')
	Pheo b (b')	Pheo b (b')	Fucoxanthin	Fucoxanthin	Fucoxanthin
	β-Carotene	β-Carotene			
Osmolytes	Glycerol	Glycerol	CHT	CHT	CHT
	Homarine		DHPS	DHPS	DMSP
			Scyllo-inositol	*Scyllo*-inositol	*Scyllo*-inositol
					Homarine
Amino acids	Ala	Ala	Ala	Ala	Ala
	Tyr	Tyr	Tyr	Tyr	Tyr
Carbohydrates			β-Glc	β-Glc	β-Glc
			α-Glc	α-Glc	α-Glc
			chrysolaminarin[b]	chrysolaminarin[b]	(1 → 3, 1 → 6)-β-D-glucan[b]
Others	Lactate	Lactate			FFA
					Squalene
					Brassicasterol
					Mannitol

TG: triacylglycerols. MGDG: monogalactosyldiacylglycerols. DGDG: digalactosyldiacylglycerols. SQDG: sulphoquinovosyldiacylglycerols. PULCA: polyunsaturated long-chain alkenones FFA: free fatty acids. Pheo: pheophytin. SAFA: saturated fatty acid. MUFA: monounsaturated fatty acid. OL: oleic acid. LO: linoleic acid. HDTA: hexadeca-4,7,10,13-tetraenoic acid. ALA: α-linolenic acid. SDA: stearidonic acid. ARA: arachidonic acid. EPA: eicosapentaenoic acid. DHA: docosahexaenoic acid. CHT: 1,4/2,5-cyclohexanetetrol. DHPS: 2,3-dihydroxypropane-1-sulfonate. DMSP: dimethylsulfoniopropionate. Glc: glucose. Ala: alanine. Tyr: tyrosine.
c. Tentative assignment.
[a] Tentatively: myristic (C14:0) and palmitic acids (C16:0).
[b] Tentatively: palmitoleic acid (C16:1).

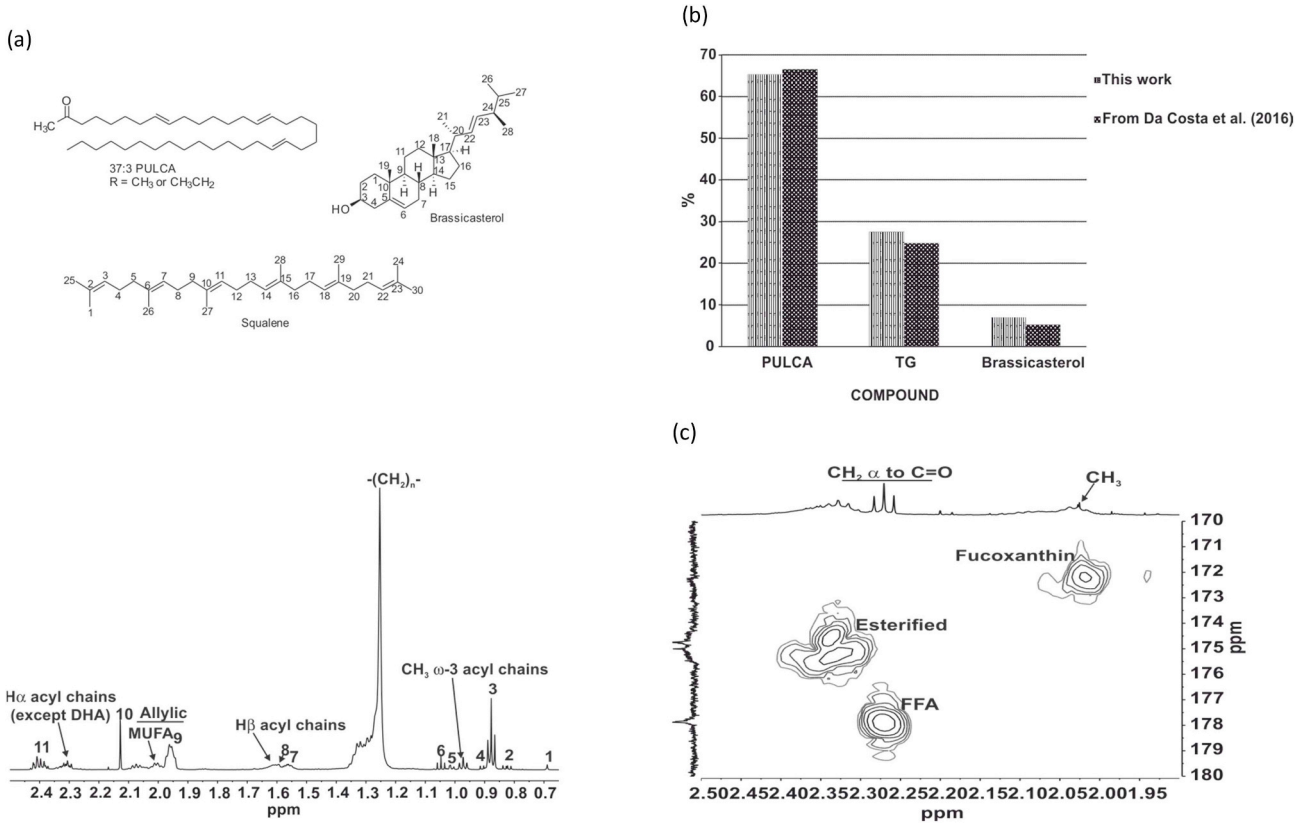

Fig. 3. NMR spectra and metabolites identified in extracts from *T. lutea*. (a) Expansion of the δ 2.50–0.65 ppm region of the 1H NMR spectrum measured in $CDCl_3$ of the hexane extract. (b) Comparison between the proportions of TGs, PULCAs and brassicasterol obtained from the NMR analysis of the hexane extract and those reported by Da Costa et al. (2016) using GC. (c) Expansion of the HMBC spectrum measured in CD_3OD of the AcOEt extract in the δ_H 2.5–1.9 ppm and δ_C 170-180 ppm regions. Signals 1, 2, 4 and 5: brassicasterol (18, 26 and 27, 28, 19 and 21, 22 and 23). Signals 3, 6, 7, 9, 10 and 11: PULCAs (terminal CH_3 overlapped with terminal CH_3 of acyl chains other that ω-3, $CH_3CH_2C{=}O$, CH_2 (long-chain) β to C=O, allylic trans, $CH_3C{=}O$, $CH_3CH_2C{=}O$ overlapped with CH_2 α to C=O of long-chain methyl, ethyl ketones and DHA). Signal 8: squalene.

showed the carbonyl resonances of the acyl chains in the range of δ 174-172 ppm (Gunstone and Seth, 1994). Other minor components present in these extracts were sterols identified through the signals that appear in the δ 0.64–0.52 ppm range assigned to the methyl group 18 (Fig. 2). Chlorophylls and carotenoids give rise to characteristic signals in the high δ region (δ 11.5–5.5 ppm) of 1H NMR spectra (Sobolev et al., 2005). Pigments were clearly identified in the NMR analyses of AcOEt extracts (see below). However, in the hexane extracts signals in this region are of very low intensity (Fig. S2), which highlights the poor ability of this solvent for extracting this type of compounds.

The 1H NMR spectrum of the hexane extract from *T. lutea* showed a clear difference with respect to the chlorophytes and the diatoms in the composition of the storage lipids. Although TGs are present, the most intense signals in this extract were due to polyunsaturated long-chain alkenones (PULCAs), in particular methyl alkenones (Fig. 3) (O'Neil et al., 2014). Biosynthesis of PULCAs is characteristic of microalgae of the haptophyte order Isochrysidales to which *T. lutea* belongs (Volkman et al., 1980; Marlowe et al., 1984; Patterson et al., 1994; Eltgroth et al., 2005). These compounds are believed to be synthesized in the chloroplast and then accumulated in cytosolic lipid bodies for storage (Patterson et al., 1994). The main components have a length chain in the range C_{37}-C_{39} with two to four double bonds with an unusual *trans*-geometry occurring at intervals of 7 carbon atoms (Rechka and Maxwell, 1987).

Polyunsaturated long-chain methyl alkenones in the strain of *T. lutea* studied here were characterized by the singlet at δ 2.13 ppm (peak 10 in Fig. 3a) that showed a cross peak in the HSQC at δ 30.0 ppm and correlated in the HMBC spectrum with a carbonyl carbon at δ 209.2 ppm. Ethyl alkenones were also detected and their relative concentration in the mixture could be estimated through the methyl protons of the CH_3CH_2CO moiety that resonated at δ 1.05 ppm isolated from other terminal CH_3 groups (peak 6 in Fig. 3a). The *trans*-geometry of the carbon-carbon double bonds in PULCAs was determined through the chemical shifts of the allylic protons that resonated at δ_H = 1.96 ppm/δ_C = 32.1 ppm (peak 9 in Fig. 3a). The methylene protons in β-position with respect to the carbonyl group of PULCAs resonated at slightly lower chemical shift than those in acyl chains of TGs (peak 7, Fig. 3a). The HSQC spectrum of the hexane extract showed the corresponding correlations with carbon atoms at δ 24 and 25 ppm for the proton signals at δ 1.56 ppm (CH_2 in β-position with respect to the carbonyl group in PULCAs) and δ 1.61 ppm (CH_2 in β-position with respect to the carbonyl group in acyl chains), respectively. Furthermore, this spectrum also showed the contribution in the signal at δ 1.61 ppm of methyl groups at δ_C 16.1 and 17.9 ppm that may arise from squalene (peak 8, Fig. 3a). A close inspection of the HSQC and HMBC spectra, together with data reported in the literature (Borchman et al., 2013), allowed confirmation of the presence of this compound in the hexane extract. Signals labeled as 1, 2, 4 and 5 in Fig. 3a were assigned to brassicasterol based on their chemical shifts and the correlations found in the HSQC and HMBC spectra, which also allowed the assignment of some additional signals of this cell membrane sterol (Table S1, Supplementary Material) (Weete et al., 1985; Sun et al., 2014). The presence of brassicasterol is a distinctive feature of *Tisochrysis* strains with respect to the closely related species *Isochrysis galbana* that contains epibrassicasterol (Patterson et al., 1994).

The relative proportions of PULCAs, TGs and brassicasterol estimated from the 1H NMR spectra of the hexane extract were comparable to the data reported for *T. lutea* (strain CCAP 927/14) by Da Costa et al.

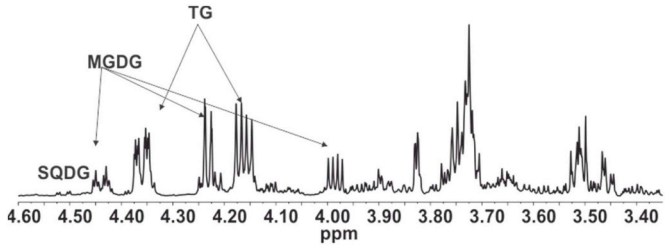

Fig. 4. Expansion of the 1H NMR spectrum, measured in CD_3OD, of the *C. calcitrans* AcOEt extract in the δ 4.60–3.35 pm region showing characteristic signals of SQDGs, MGDGs and TGs.

(2016) using GC (Fig. 3b). These authors also found minor amounts of free fatty acids (FFA). FFA were clearly identified in the AcOEt extract through the resonances due to methylene protons in α-position with respect to the carbonyl group (Fig. 3c). This similitude in chemical composition reflects the phylogenetic proximity between the strains (Bendif et al., 2013).

In general, structural membrane lipids, mainly MGDGs, were the major lipids identified in AcOEt extracts (Figs. S5–S7). The *C. calcitrans* strain was the exception. As can be observed in Fig. 4 the 1H NMR spectrum of the AcOEt extract for this strain showed a preponderance of TGs over MGDGs, whereas for the other extracts resonances due to storage lipids were almost absent. This result indicates that accumulation of TGs in *C. calcitrans* was much higher than in the other strains. As a result, under the experimental conditions used their complete extraction in the hexane fraction was not possible.

Although MGDGs preponderate among structural membrane lipids, inspection of the 2D NMR spectra allowed the detection of minor amounts of DGDGs and SQDGs. The 1H and 13C chemical shifts for these compounds (Table S1) were similar to published data (Logvinov et al., 2015).

Pigments were concentrated in AcOEt extracts and two types of pigments were identified in the microalgae studied: chlorophylls detected as pheophytins due to the pheophytinisation process during extraction (Pollesello et al., 1992) and carotenoids. Chlorophylls (Chl) and chlorophyll derivatives can easily be identified by 1H NMR spectroscopy due to the isolated proton resonances between δ 11.2 and 8.5 ppm (Abraham and Rowan, 1991). Thus, the singlets at δ 9.53, 9.40 and 8.55 ppm that correlated in the HSQC spectrum with carbon resonances at δ 104.6, 97.8 and 93.2 ppm, respectively, were assigned to pheophytin *a* (Pheo *a*). Pheophytin *b* (Pheo *b*) was identified by the resonances at δ_H 11.16/δ_C 188.2 ppm and δ_H 10.05 and 9.77 ppm (Fig. 5a). Minor amounts of the *a'* and *b'* isomers were also clearly identified (Table S1).

Among chlorophylls, Chl *a* is the major and most important component found in phothosyntetic organisms, whereas Chl *b* is only found in green lineage. In agreement with this, the 1H NMR spectrum of the AcOEt extract for the five studied strains showed the presence of Pheo *a* (*a'*), whereas Pheo *b* (*b'*) was only found in the *Dunaliella* strains.

The ability of *Dunaliella* to adapt to a broad range of environmental conditions through accumulation of β-carotene is well known, whereas the xanthophyll fucoxanthin is the main carotenoid present in diatoms and haptophytes (Peng et al., 2011; Kuczynska et al., 2015; Mulders et al., 2013; Serive et al., 2017). The terpenic chain of carotenoids appeared between δ 6.7 and 6.0 ppm. The unambiguous identification of β-carotene in the non-polar fraction of *Dunaliella* sp. and *D. salina* was possible based on the analysis of the 2D NMR spectra in combination with reported data (Tsukida et al., 1981). The allenic nature of fucoxanthin and the presence in its carbon skeleton of conjugated carbonyl, epoxide and acetyl groups facilitated the NMR identification (Fig. 5b) (Englert et al., 1990). The olefinic proton H10 of fucoxanthin appeared in the 1H NMR spectrum as a highly deshielded doublet (δ 7.13 ppm, J = 11.1 Hz) due to the conjugation with the carbonyl group

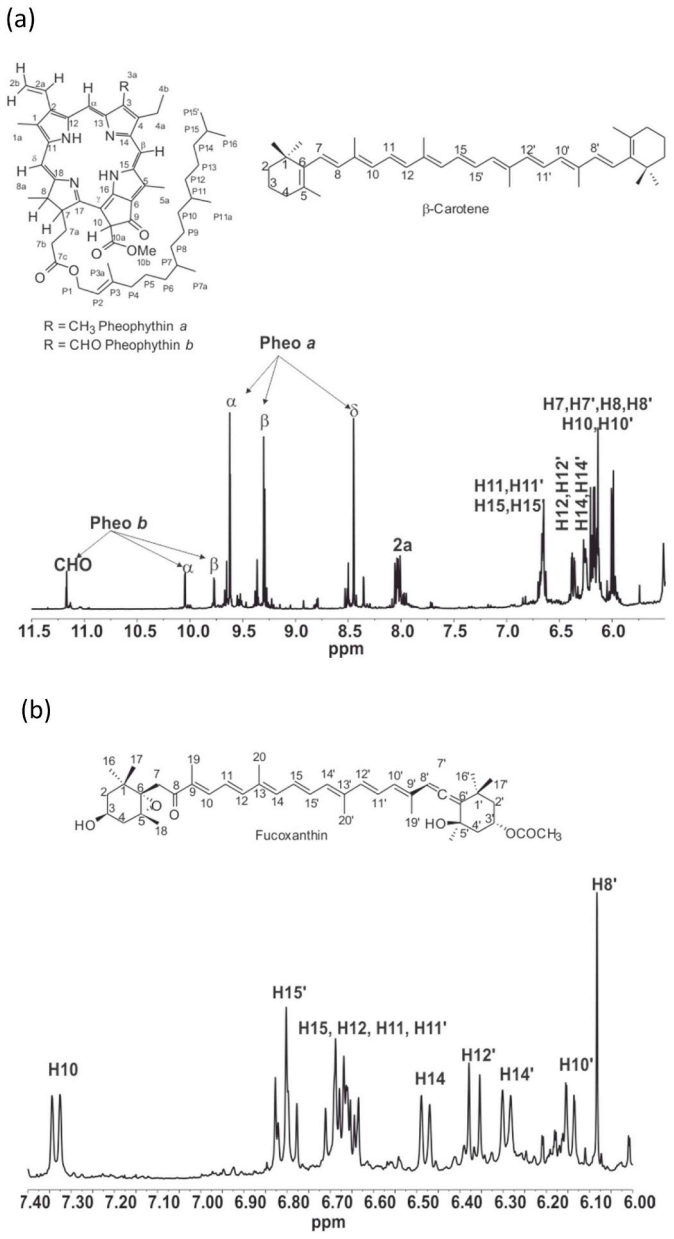

Fig. 5. Expansions of the 1H NMR spectra measured in CD_3OD of AcOEt extracts from (a) *Dunaliella* sp. (δ 11.50–5.50 ppm region) and (b) *C. calcitrans* (δ 7.20–5.80 ppm region).

and correlated in the HMBC spectrum with the carbonyl signal at δ 197.9 ppm. On the other hand, the singlet at δ 6.05 ppm (H8′, Fig. 5b) showed a correlation in the HSQC spectrum with the carbon resonance at δ 103.5 ppm, as well as correlations in the HMBC spectrum at δ 202.2 and 117.0 ppm that confirmed the allenic nature of this proton. Additional correlations found in the HMBC spectrum corresponding to C10′(δ 128.6 ppm) and C19' (δ 14.2 ppm) supported this assignment. The absence of acetylation at C3 was indicated by the chemical shifts of the proton and carbon at this position δ_H = 5.38 ppm/δ_C = 68.2 ppm. Other proton signals of this compound appeared overlapped with those of MGDGs, the major components of the ethyl acetate extract. Notwithstanding, the complete assignment of fucoxanthin was possible through the analysis of the HSQC and HMBC spectra (Table S1). Fucoxanthin was also the only carotenoid found in the haptophyte *T. lutea*.

Besides structural membrane lipids and pigments, glycerol was clearly detected in the AcOEt extracts of *Dunaliella* strains (Fig. 6). The relative amount of glycerol present in the AcOEt extracts from the two

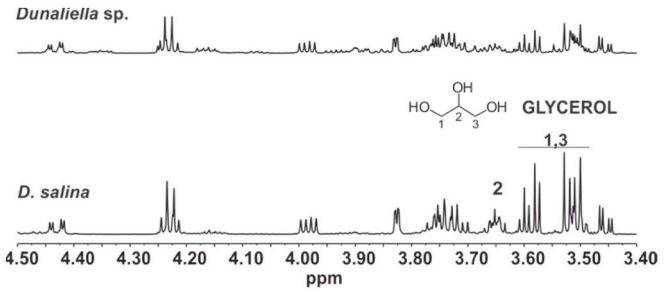

Fig. 6. Expansion of the 1H NMR spectra measured in CD_3OD of AcOEt extracts from *Dunaliella* sp. (top) and *D. salina* (bottom) in the δ 4.50–3.40 ppm region.

strains was different. Thus, it was the major component of the *D. salina* AcOEt extract, whereas in *Dunaliella* sp. MGDGs preponderated (MGDG:glycerol 1:1.1 and 1.7:1 for *D. salina* and *Dunaliella* sp. AcOEt extracts, respectively). This compound is a photosynthetic product of *Dunaliella* and is also formed by the degradation of starch, the storage product in this microalga (Ben-Amotz and Avron, 1973). The lack of a rigid cell wall is a morphological characteristic of species in this genus and the formation and degradation of glycerol constitutes the main mechanism for the regulation of the osmotic pressure within the cells.

2.1.2. Fatty acid distribution

Fatty acid composition from microalgae has been extensively analyzed by chromatographic techniques (Yao et al., 2015). The content of fatty acids may vary between species of the same genus and even between isolates of a single species. However, the distribution pattern of fatty acids provides, in general, a clear differentiation between phyla, classes and genera of microalgae. In Chlorophyta, the frequency of ARA (C20:4 ω-6), EPA (C20:5 ω-3) and DHA (C22:6 ω-3) fatty acids has been reported to be very low (Lang et al., 2011). The genus *Dunaliella* is not an exception. Although the content and proportion of fatty acids depend on specific growth conditions (nutrient levels, temperature, light intensity, salinity) (Abd El-Baky et al., 2004; Roleda et al., 2013; Kim et al., 2015), the pattern is common for different species in this genus with the ω-3 PUFAs hexadeca-4,7,10,13-tetraenoic acid (HDTA, C16:4) and α-linolelic acid (ALA, C18:3) as the major components (Volkman et al., 1989; Viso and Marty, 1993; Zhukova and Aizdaicher, 1995). The high proportion of these two fatty acids is considered distinctive for marine microalgae of the class *Chlorophyceae* within the division Chlorophyta (Viso and Marty, 1993; Zhukova and Aizdaicher, 1995). In contrast, diatoms are an important source of EPA and ARA. Another abundant PUFA found in these microalgae is the ω-4 fatty acid C16:3, but the amount of C18 fatty acids was very low (Volkman et al., 1989; Viso and Marty, 1993; Zhukova and Aizdaicher, 1995; Dunstan et al., 1994; Miller et al., 2014). In *C. calcitrans* C16:3 ω-4 fatty acid seems to be present predominantly in the glycolipid fraction, whereas EPA is stored as TG (Miller et al., 2014).

NMR analysis of the hexane and ethyl acetate extracts from the strains studied here were consistent with the reported fatty acid distributions. Furthermore, from the analysis of the 13C NMR and 2D 1H, 13C HMBC spectra the positional distribution of the acyl chains on the glycerol moiety can be obtained. Composition of storage lipids can differ from that of membrane lipids (Millar et al., 2000) and the NMR approach also allows their discrimination.

Inspection of the δ 3.0–0.7 ppm region of the 1H NMR spectra of the ethyl acetate extracts from *Dunaliella* sp. and *D. salina* (Fig. S5) indicated the same distribution of acyl chains in MGDGs. Analysis of the 13C NMR spectrum of the *Dunaliella* sp. AcOEt extract (Fig. 7, Table 2) confirmed that the main ω-3 PUFAs produced by this microalgae are the expected C18:3 and C16:4. The carbonyl signal with the highest chemical shift was assigned to the α-linolenate (ALA) attached to the *sn*1 position of glycerol in MGDGs by comparison with published data (Sakano et al., 2005). The esterification position of this chain was

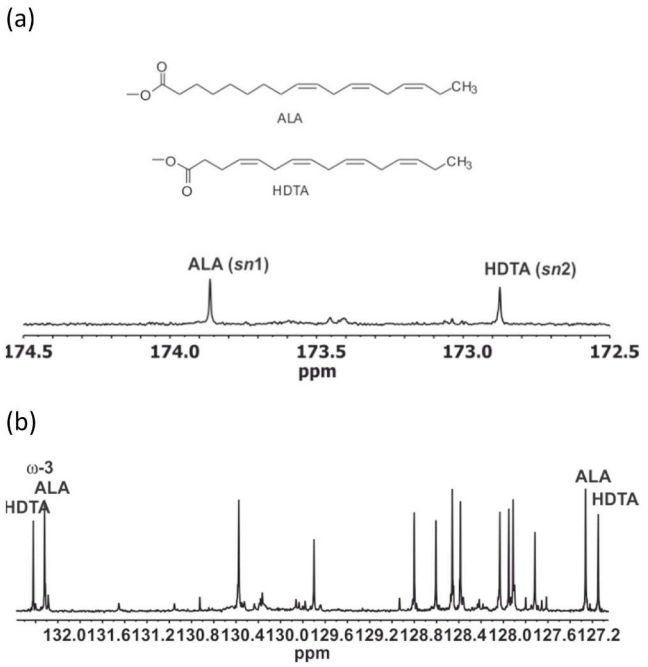

Fig. 7. Expansions of the 13C NMR spectrum of the AcOEt extract from *Dunaliella* sp. measured in $CDCl_3$: (a) carbonyl and (b) olefinic region.

Table 2
13C NMR chemical shifts of linolenate (ALA, C18:3) and hexadeca-4,7,10,13-tetraenate (HDTA, C16:4) in MGDG. Chemical shifts are reported with respect to $CDCl_3$ (δ 77.16 ppm).

	ALA	HDTA
C1	173.86 (*sn*1)	172.87 (*sn*2)
C2	34.27	34.23
C3	24.96	Allylic
C4	29.34	Olefinic
C5	29.28	
C6	29.24	
C7	29.75	
ω-1	14.42	14.42
Allylic		
ω-2	20.70	20.71
Other	27.36 (C8)	22.78 (C3)
Bisallylic		
	25.77	25.77[a]
	25.68	
Olefinic		
ω-3	132.12	132.22
ω-4	127.26	127.15
Other	130.39; 129.70; 128.82; 128.61; 128.46; 128.39; 128.03; 127.95; 127.91; 127.72	

[a] This signal represents the three bisallylic carbons present in the chain.

confirmed by the HMBC spectrum through correlation between the carbonyl resonance and the *sn*1 protons of the glycerol backbone in MGDGs (δ 4.40 and 4.20 ppm). Analogously, the carbonyl resonance at δ 172.87 ppm was assigned to HDTA esterified to the *sn*2 position of the glycerol in MGDGs based on correlation with protons at δ 5.30 ppm and 2.38 ppm. This result is in agreement with the classification of *Dunaliella* microalgae as "16:3 plants" in which the galactolipids are mainly composed by one polyunsaturated acid of 18 carbon atoms and one polyunsaturated acid of 16 carbon atoms (Thompson, 1996).

The fatty acid composition of TGs in the two strains of *Dunaliella* was, however, clearly different (Fig. S2). Polyunsaturated acyl chains were almost absent in the storage lipids produced by *D. salina*. For this strain SAFA and MUFA in approximately 1:1 ratio preponderated. In contrast, acyl chains attached to glycerol backbone of TGs in *Dunaliella*

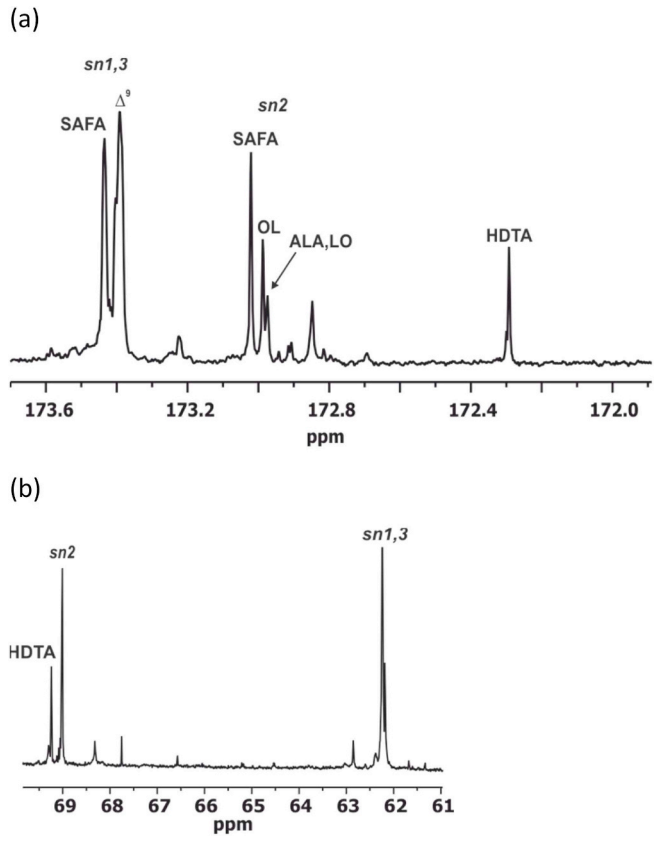

Fig. 8. Expansions of the 13C NMR spectrum of hexane extract from *Dunaliella* sp. measured in $CDCl_3$: (a) carbonyl region and (b) the *sn*2 and *sn*1,3 regions.

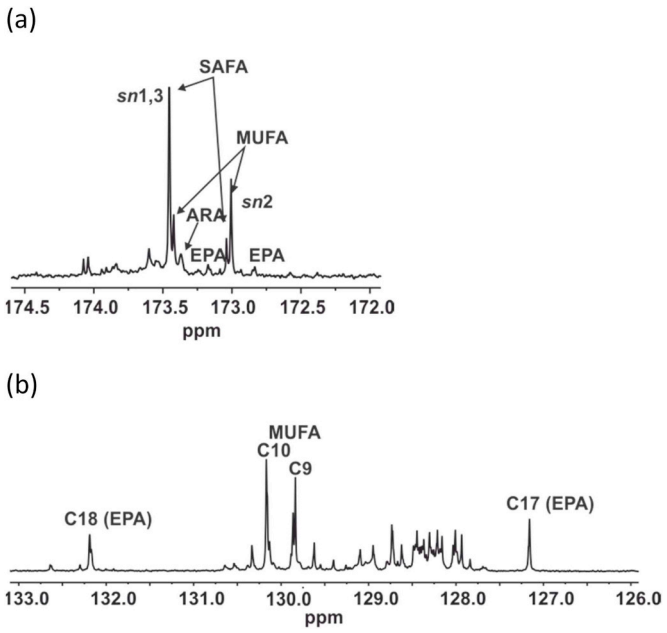

Fig. 9. Expansions of the 13C NMR spectrum of the hexane extract from *C. calcitrans* measured in $CDCl_3$: (a) carbonyl and (b) olefinic regions.

sp. were more complex as deduced from the higher number of signals in the carbonyl region of the 13C NMR spectrum of the hexane extract (Fig. 8a). The assignment of the signal at δ 172.29 ppm to HDTA is confirmed by the correlation in the HMBC spectrum with the proton resonance at δ 2.39 ppm (CH_2 in α and β positions with respect to C═O). However, in this case the HMBC spectrum did not provide unambiguous information about the position (*sn*1,3 or *sn*2) of esterification. Fortunately, inspection of the glyceryl region of the 13C NMR (Fig. 8b) allowed verification that esterification of HDTA occurs exclusively at the *sn*2 position. In fact, the deshielding of the signal assigned to the *sn*2 carbon esterified with HDTA (0.23 ppm) was consistent with the increase in chemical shift between Δ^4 and other acyl chains reported in the literature (Sacchi et al., 1993).

The other signals for the carbonyl carbons in TGs fell in two groups separated by ca. 0.4 ppm corresponding to acyl chains esterified to the *sn*1,3 and *sn*2 positions of the glycerol (Gunstone, 1990; Diehl et al., 1995) (Fig. 8a). Three signals were clearly observed in the *sn*2 region that were assigned by comparison with literature data (Sacchi et al., 1993; Salinero et al., 2012) to carbonyl carbons of saturated (δ 173.02 ppm), oleyl (OL, C18:1) and linoleyl (LO, C18:2, δ 172.99 ppm) and linolenyl, ALA, (δ 172.97 ppm) acyl chains (Fig. 8a). Although the effect of the Δ^9 double bond in LO and ALA on the carbonyl chemical shift is the same, some spectral features support their presence: proton resonance for the bisallylic methylene in LO at δ 2.76 ppm and the characteristic signals for the olefinic ω-3 and ω-4 carbons of ALA at δ 132.08 and 127.25 ppm, respectively. Taking into account the proportion of ω-3 acyl chains in this microalgae, linolenyl ester should be the main contributor to the δ 172.97 ppm signal. The carboxyl and glycerol regions of the 13C NMR spectra (Fig. 8a and b, respectively) highlighted the non-symmetric structure of the triacylglycerols.

In the *Chaetoceros* strains, the NMR analysis of the hexane extracts revealed that SAFA and MUFA are the major acyl chains attached to the glycerol in TGs (Figs. 9 and S3). The shape of the signal due to the allylic protons (Fig. S3) and the intensity of the olefinic carbons with the major signals at ca. δ 130 and 129 ppm corresponding to the C10 and C9 carbon atoms of MUFA (Fig. 9b) showed that monounsaturated acyl chains preponderated over polyunsaturated acyl chains. Splitting of these olefinic carbons into two signals with a separation of 0.02 ppm for C9 and 0.01 ppm for C10 was clearly observed. These two signals correspond to the presence of monounsaturated acyl chains attached to the *sn*1,3 and *sn*2 position of glycerol in TGs, δ 129.86 (C9)/130.17 (C10) and 129.84 (C9)/130.16 (C10) ppm, respectively (Gunstone, 1990; Diehl et al., 1995) (Fig. 9b). In light of the major fatty acids found in diatoms, these signals might be due to palmitic (C16:0), myristic (C14:0) and palmitoleic (C16:1, ω-7) acids (Volkman et al., 1989; Viso and Marty, 1993; Zhukova and Aizdaicher, 1995; Dunstan et al., 1994; Miller et al., 2014). The preponderance of both saturated and monounsaturated acyl chains was clearly established based on the lowest field signals of the 13C NMR spectrum (Fig. 9a, Table S1).

EPA and ARA can easily be identified by 1H NMR spectroscopy through the resonance of the methylenic protons in β-position with respect to the carbonyl group (Fig. S6). These protons are also in β-position to a double bond and thus resonates ca. 0.12–0.08 ppm downfield from those of other acyl chains (Vidal et al., 2012). The lack in the 1H and 13C NMR spectra of characteristic signals for Δ^4 (δ_H 2.42–2.36 ppm) and ALA (δ_C 132.1 and 127.3 ppm) acyl chains allowed assignation the triplet at δ 0.95 ppm to the terminal methyl group of EPA. The integration of this signal and that corresponding to the methylenic protons in β-position with respect to the carbonyl group provided an estimation of the relative proportion of EPA and ARA. The values obtained indicated that this strain of *C. gracilis* does not accumulate ARA as TGs. In the case of *C. calcitrans* and taking into account that TGs preponderate in both the hexane and the AcOEt extracts, the results suggest that this strain stores, as TG, approximately twice as much EPA as ARA.

In the AcOEt extracts ω-4 acyl chains were also unambiguously identified in both strains of *Chaetoceros* and thus they should be mainly present as MGDGs (Fig. S6). Miller et al. (2014) also found a high amount of C16:3 ω-4 in a GC analysis of the fatty acid distribution in the glycolipid fraction of *C. calcitrans*. The high field region of the 1H NMR spectrum of the ethyl acetate extract showed the presence of a triplet at

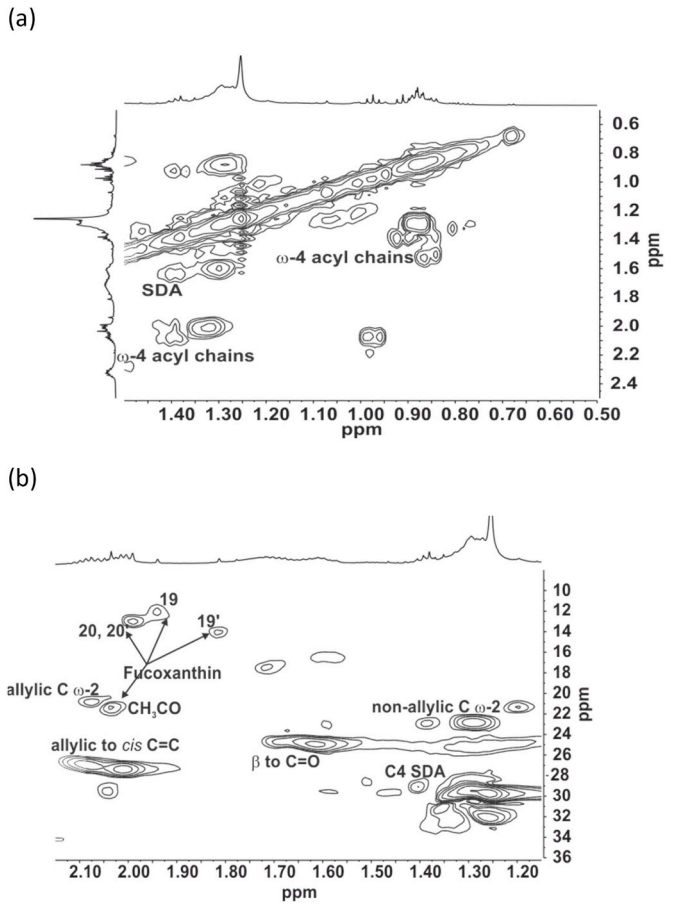

Fig. 10. Expansions of 2D NMR spectra of AcOEt extracts from *C. calcitrans* measured in $CDCl_3$: (a) COSY spectrum showing the correlations of the methyl and methylene protons of ω-4 acyl chains; (b) HSQC spectrum (δ_H 2.15–1.15 ppm and δ_C 36-8 ppm regions).

δ 0.91 ppm that correlated in the HSQC spectrum with a carbon at δ 13.95 ppm. The assignment of this signal to the terminal methyl group of ω-4 acyl chains was confirmed through the correlations found in the COSY spectrum. Thus, the triplet at δ 0.91 ppm correlated with the multiplet centered at δ 1.38 ppm that, in turn, also showed correlation with allylic protons at δ 2.10 ppm (Fig. 10a). Furthermore, a second correlation between the signal at δ 1.38 ppm and the resonance of methylene protons in β-position to the carbonyl group (δ 1.60 ppm) indicated the presence of acyl chains of stearidonic acid (SDA) (Dais et al., 2015). Biosynthesis of SDA in *Chaetoceros* strains was confirmed by the HSQC spectrum (Fig. 10b). Thus, the multiplet at δ 1.38 ppm corresponding to a CH_2 group showed cross peaks at about δ 23 and 24 ppm, in the typical range of non-allylic ω-2 and C4 carbon resonances of unsaturated acyl chains, respectively. Signals at δ 0.91 and 1.38 ppm have been found in NMR analyses of fish oil supplements and they have been assigned also to ω-4 acyl chains but with a trans geometry of the double bond. However, no unequivocal support for this assignment was given (Dais et al., 2015). Detection of *trans*-fatty acid chains can be achieved through the chemical shifts of allylic carbons. The *trans*-geometry of the double bond increases the carbon chemical shift of the allylic methylenic carbons that resonate in the δ 32.7–32.5 ppm range (Sacchi et al., 1997). There was no correlation in the HSQC spectrum between the allylic protons and carbon resonances in the expected range for methylene groups adjacent to a trans double bond (Fig. 10b).

Despite the overlap between the proton resonances of the acyl chains in TGs and PULCAs, acyl chains corresponding to the major fatty acids reported in *T. lutea* could be determined by NMR. Oleic acid was

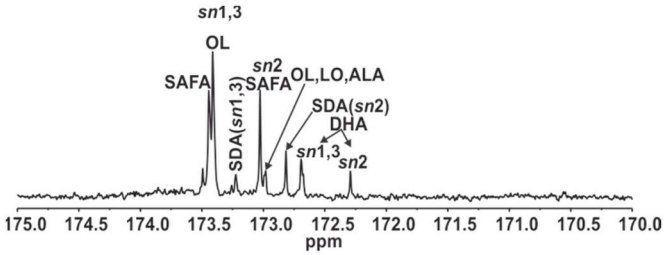

Fig. 11. Expansion of the carbonyl region of the 13C NMR measured in $CDCl_3$ of the hexane extract from *T. lutea*.

clearly identified in the 1H NMR spectrum by the characteristic resonance of the allylic protons (Fig. 3a). Furthermore, the carbonyl resonance of this acyl chain esterified to the *sn*1,3 positions of the glycerol in TGs (δ 173.41 ppm) besides those of SAFA attached to the *sn*1,3 and *sn*2 positions (δ 173.44 and 173.03 ppm, respectively) were the most prominent signals in the δ 174-172 ppm region of the 13C spectrum (Fig. 11). The two carbonyl resonances at the lowest chemical shift separated by 0.40 ppm indicated the presence of DHA attached to both the *sn*2 (δ 172.29 ppm) and *sn*1,3 (δ 172.69) positions of glycerol. The correlation with the proton signal at δ 2.39 ppm in the HMBC spectrum confirmed this assignment. Stearidonic acid (C18:4 ω-3) was also identified through the carbonyl resonances at δ 172.82 (*sn*2) and 173.22 (*sn*1,3) ppm (Fig. 11). It has been reported that in *T. lutea* LO and ALA contribute ca. 4% and 6%, respectively to total fatty acid content (Da Costa et al., 2016). Minor signals characteristic of these acyl chains were also detected in the NMR spectra. On the other hand, the lack of EPA corroborates again the phylogenetic separation between *T. lutea* and *I. galbana* (Liu and Lin, 2001).

2.1.3. Polar metabolites

Although the most polar lipids (DGDGs and SQDGs) were detected in the AcOEt extract, the polarity of this solvent is not sufficient for their complete extraction. As a result, they appeared also in the methanolic extracts. However, in all cases osmolytes were the major compounds present in these extracts. Thus, the most prominent signals in the 1H NMR spectra of methanolic extracts from *Dunaliella* corresponded to glycerol (Fig. S8). Glycerol was not detected in the other three strains in which 1,4/2,5-cyclohexanetetrol (CHT) was the major polyol (Fig. 12). This compound was characterized by the proton signals at δ 3.73 and 1.83 ppm that showed correlations in the HSQC spectrum at δ 71.6 (CH) and 35.3 (CH_2) ppm, respectively (Maras et al., 1998; Kobayashi et al., 2007; Garza-Sánchez et al., 2009). *Scyllo*-inositol was also identified in the *Chaetoceros* and *T. lutea* strains (Fig. 12). The six methinic groups in this stereoisomer of *myo*-inositol are equivalent and appeared at δ_H 3.21 ppm and δ_C 75.5 ppm. This cyclitol has been described in the haptophyte *Pavlova sp.* (Kobayashi et al., 2007) and in the diatom *Phaeodactylum tricornutum* (Ford and Percival, 1965). Cyclitols are organic osmolytes, i.e. small solutes that maintain cell volume and fluid balance and regulate plant responses to multiple stresses (Yancey, 2005). Thus, in chromalveolates (*Chaetoceros, Pavlova, Boekelovia, Nitzschia*) 1,4/2,5-cyclohexanetetrol acts as an osmoregulator and its proportion increases when the algae are subjected to salinity stress (Fujii et al., 1995; Kobayashi et al., 2007; Garza-Sánchez et al., 2009). In contrast, changes in the amount of *scyllo*-inositol in response to external salinity has not been observed in *Pavlova sp.* (Kobayashi et al., 2007). Furthermore, mannitol, one of the most abundant natural polyols, was also identified in the methanolic extract from *T. lutea* (Fig. 12). This compound can play various important physiological roles such as carbon storage and protection against environmental stress. In alkenone producing strains, both alkenones and mannitol seems to be the major carbon/energy storage compounds (Obata et al., 2013; Tsuji et al., 2015).

Dimethylsulfoniopropionate (DMSP) (Obando et al., 2016) was,

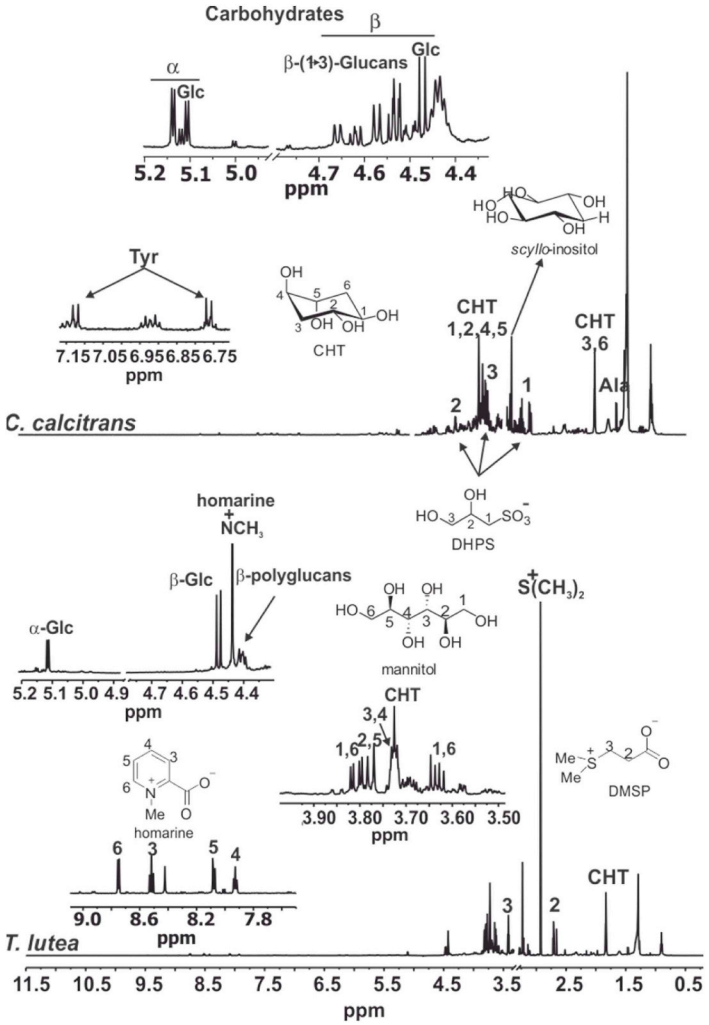

Fig. 12. 1H NMR spectra of the MeOH extracts measured in CD_3OD from the diatom *C. calcitrans* (top) and the haptophyte *T. lutea* (bottom).

together with CHT, the most abundant metabolite found in the *T. lutea* methanolic extract (Fig. 12). The function of DMSP as an osmoprotector in microalgae is well known and its production seems to be taxon-dependent, with *Dinophyceae* and *Prymnessiophyceae* being major sources of this compound (Keller et al., 1999). DMSP can also act as an antioxidant and predator repellent (Yancey, 2005). Furthermore, DMSP, produced by phytoplankton in response to different environmental stresses, is the primary precursor of dimethylsulfide (DMS) and thereby has important roles in the biogeochemistry and ecology in marine microbial communities (Kiene et al., 2000).

DMSP was not detected in the studied strains of *Chaetoceros*. However, the presence of a methylene attached to a sulfonyl group in the 1H NMR spectrum of their methanolic extracts was deduced from the double doublets at δ 3.05 (J = 14.1 Hz, 4.2 Hz) and 2.90 (J = 14.1 Hz, 7.9 Hz) ppm (Fig. 12) that showed a correlation in the HSQC spectrum with the carbon resonance at δ 55.1 ppm. This signal correlated in the HSQC-TOCSY spectrum with another methylene group at δ_H 3.63 and 3.58 ppm/δ_C 66.2 ppm and a methine group at δ_H 4.12 ppm/δ_C 69.7 ppm. These NMR data are consistent with those reported for 2,3-dihydroxypropane-1-sulfonate (DHSP) identified as one of the metabolites formed during the bacterial degradation of sulfoquinovose, the headgroup of SQDG (Roy et al., 2003). DHSP has been also identified in cells of the fresh-water diatom *Navicula pelliculosa* (Busby, 1966). More recently, Durham et al. (2015) reported the occurrence of significant intracellular concentrations of this compound in diatoms. From the study of co-cultures of the diatom *Thalassiosira pseudonana* and the marine bacteria *Ruegeria pomeroyi*, these authors concluded that DHSP released by the diatom is subsequently used as a major substrate for the bacteria underlying the important role of this sulfonate as a reservoir of carbon and sulfur in the ocean.

Minor amounts of the quaternary ammonium compound homarine, unambiguously identified by 1H NMR through the aromatic protons resonating in the low-field region of the spectrum (Affeld et al., 2006; Gebser and Pohnert, 2013) (Figs. 12 and S8), were found in the methanolic extracts from *T. lutea* and *Dunaliella* sp. but this metabolite was not detected in either *D. salina* nor *Chaetoceros* strains.

On the other hand, for the five studied strains, the 1H NMR spectra of the methanolic extracts also showed relatively weak signals of the amino acids alanine (Ala) and tyrosine (Tyr). Carbohydrates were also detected except in the *Dunaliella* strains, in which amounts of lactate were in turn found (Fig. S8). The occurrence of carbohydrates was shown by the presence of a set of doublets due to anomeric protons in β- (δ 4.67–4.37 ppm, $J \approx 8$ Hz) and α-hexapyranoses (δ 5.16–5.10 ppm, $J \approx 3.7$ Hz) (Fig. 12). The two epimers of D-glucose were unambiguously identified through the doublets at δ 4.48 ppm (J = 7.8 Hz) and 5.11 ppm (J = 3.7 Hz) corresponding to the anomeric protons of β- and α-glucose, respectively, by comparison with a sample of standard glucose measured in methanol-d_4.

Glucose is the major sugar reported in the polysaccharide fraction of *C. calcitrans* (Brown, M.R., 1991). This sugar arises from the β-(1 → 3)-glucan named chrysolaminarin that is the main storage product of photosynthetic CO_2 fixation in diatoms. Chrysolaminarin is a relatively

short-chained glucose polymer very soluble in water/methanol that is included in the low molecular weight fraction (Granum and Myklestad, 2001). The HSQC spectrum showed correlations between the proton signals in the β-anomeric region with carbons in the range corresponding to non-reducing sugars (δ 104.5 ppm). The glycosidic linkage between positions 1 and 3 was deduced from the correlation found in the HMBC spectrum between the anomeric protons with carbon signals at δ 83.3 and 87.0 ppm. These data are in agreement with the presence of β-(1 → 3)-glucans in the methanolic extract and may correspond to different glucopyranosyl units of these polysaccharides (Størseth et al., 2004, 2006). On the other hand, the presence of non-reducing sugars with α configuration other than α-glucose was revealed by the correlations, in the HSQC spectrum, between the doublets at δ 5.14 (J = 3.6 Hz) and 5.12 (J = 3.8 Hz) and carbons at δ 93.4 and 93.6 ppm, respectively. Furthermore, the signal at δ 5.14 ppm showed a correlation in the HMBC with a carbon resonance at δ 84.2 ppm suggesting a glycosidic linkage in a position different to the anomeric one. However, the complexity of the mixture precludes an unambiguous assignment for this signal.

In the methanolic extract of *T. lutea* the anomeric protons of β-hexapyranoses other than β-glucose appeared between δ 4.41 and 4.37 ppm as a set of overlapping doublets with coupling constants of ca. 8 Hz (Fig. 12, Table S1). These signals showed correlations, in the HSQC spectrum, with carbon resonances at δ 103.7 ppm and in the COSY spectrum with protons at δ 3.25 ppm. In turn, the HMBC spectrum showed two correlations between these anomeric protons and carbon signals at δ 75.9 and 69.4 ppm. These results indicate the presence of units of β-glucose with a glycosidic linkage between the positions 1 and 6. Although the nature of carbohydrates in *T. lutea* is not well known (Garnier et al., 2016), the results suggest the presence of highly branched (1 → 3, 1 → 6)-β-D-glucan probably similar to that reported for *Isochrysis galbana* with potential antitumor activity (Sadovskaya et al., 2014).

2.2. Bioactivity studies

The antimicrobial activity of crude extracts from microalgae has usually been attributed to the presence of compounds with well-known activity (Herrero et al., 2006; Mendiola et al., 2007, 2008). The compositional study of the five strains investigated here (Table 1) showed the presence in these microalgae of several compounds with potential antibacterial and, possibly also, antibiofilm activities. For example, acyl chains of unsaturated fatty acids (palmitoleic, OL, LO, ALA, DHA, EPA) that have been reported to have antibiotic effect (Ohta et al., 1995; Zheng et al., 2005; Desbois and Mearns-Spragg, 2009; Ruffell et al., 2016) were found. In invertebrates, homarine acts as an antipredatory and antifouling agent. It has been reported (Slattery et al., 1997) that the soft coral *Gersemia antarctica* releases a mixture of organic compounds that confer a high antibacterial activity to the seawater around it, homarine being responsible for most of such bioactivity. On the other hand, the carotenoid fucoxanthin has been found associated with the surface of the macroalgae *Fucus vesiculosus* acting as an inhibitor of the settlement of bacteria on its surface (Saha et al., 2011).

In the present study, however, all extracts were inactive in the antibiotic bioassays for the three microorganisms tested (*Staphylococcus aureus*, *Escherichia coli* and *Candida parapsilosis*), as no growth inhibition were generated when culturing these pathogens in the presence of diverse increasing concentrations of the corresponding extracts (see section 4.3). Two human and animal pathogenic bacteria and one fungus with different resistance profiles were used: clinical isolates of *E. coli* AR (resistant to ampicillin, erythromycin, kanamycin and tetracycline), *S. aureus* S54F9 (resistant to erythromycin and kanamycin) and *C. parapsilosis* SMI416 (resistant to fluconazole). The presence of these resistance profiles may explain the difficulties in finding novel antimicrobial compounds against these three pathogens. The lack of antimicrobial activity against *E. coli* and *S. aureus* found here for the *D. salina* extracts clearly differs from the reported activity using pressurized liquid extraction (Herrero et al., 2006) or sub- and supercritical fluid extraction (Mendiola et al., 2008). This microbial activity was mainly attributed to compounds related to carotenoid degradation (α- and β-ionone, β-cyclocitral) as well as derived from galactolipid and chlorophyll catabolism (free fatty acids and phytol) due to the extraction method and conditions used. As discussed above, the precursors of such compounds (β-carotene and galactolipids) were found in extracts from *D. salina* but compounds arising from their degradation were not detected. These results suggest, therefore, that *D. salina*, in the culture conditions used in the present work, is not able to biosynthesize antibacterial compounds itself but the appropriate treatment of the extracts could transform the original secondary metabolites into potential antimicrobial substances.

The potential of the studied extracts to inhibit biofilm was also tested against nine different microorganisms causing clinical infections. They include species of the three major groups involved in human infections, Gram-positive (*S. aureus*, *Coagulase-negative Streptococcus* (*CNS*) and *S. epidermidis*), Gram-negative (*E. coli, Klebsiella pneumonia*, *E. cloacae* and *Pseudomonas aeruginosa*) and fungi (*C. albicans* and *C. parapsilosis*). The strains were selected on the basis of their resistance profile towards clinical treatments (Table 3) and ability to form biofilms.

Only the ethyl acetate extract from *C. gracilis* presented moderate antibiofilm activity against *Candida* species showing a > 4 fold-decrease in OD in comparison with the value obtained in the positive control, and presenting MBIC values of 16 mg/L and 32 mg/L for *C. albicans* and *C. parapsilosis*, respectively (Table 4). The difference between these values and those obtained for the same extract from *C. calcitrans* should be underlined. Based on the NMR data for these two extracts, the composition of pigments and MGDGs is expected to be the same for both strains. However, in *C. calcitrans* TGs were the major components of the AcOEt extract. These compounds, according to the MBIC values of the hexane extract, do not show antibiofilm activity. Recently, Lauritano et al. (2016) reported antibiofilm activity against *S. epidermis* in two marine Bacillariophyta microalgae of the Chaetocerotales order (to which *Chaetoceros* belongs). The activity was shown to be dependent on culture conditions but no compositional data of the extracts were given. Although the biofilm inhibition ability found in *C. gracilis* in our study was low, it must be stressed that the bioassays were carried out on crude extracts, i.e, a very complex mixture of metabolites. Diatoms from the order Chaetocerotales would appear to be good candidates for further investigation of potential antibiofilm activity.

3. Conclusions

NMR analyses of sequential hexane, ethyl acetate and methanol

Table 3
Selected strains for antibiofilm assays and their resistance profile.

Strain	Resistance Profile
Gram-positive	
S. aureus RPG2A	VA, LEV, CIP DO, TOB, RDS
S. epidermidis FG013	AK, VA, LEV, CIP TOB, RDS
CNS S13	AK,VA, LEV, CIP DO, TOB, RDS
Gram-negative	
E. coli 15101	LEV, CIP, TOB
K. pneumoniae AT	AK,VA, LEV, CIP, TOB
E. cloacae 6163	AK,VA, LEV, CIP, TOB
P. aeruginosa AB	VA, LEV, CIP,RD
Fungi	
C. albicans 162288680	FCA, VOR, CAS
C. parapsilosis SMI1416	AmB, FCA, VOR

AK, amikacyn; VA, vancomycin, LEV, Levofloxacin; CIP, ciprofloxacin; DO, doxycycline; TOB, tobramycin; RD, rifampicin; AmB, amphotericine; FCA, fluconazole; VOR, voriconazole; CAS, caspofungin.

Table 4
Minimal biofilm inhibitory concentrations (MBICs) in mg/L obtained.

		Dunaliella		*Chaetoceros*		*Tisochrysis lutea*
		sp.	*salina*	*calcitrans*	*gracilis*	
Hexane	*C. albicans*	512	32	256	256	64
	C. parapsilopsis	> 1024	128	> 1024	256	1024
	E. coli	> 1024	1024	> 1024	1024	1024
	CNS	> 1024	256	> 1024	256	512
	E. cloacae	512	256	> 1024	512	512
	K. pneumoniae	> 1024	1024	> 1024	1024	1024
	S. aureus	> 1024	512	> 1024	512	512
	S. epidermidis	> 1024	1024	> 1024	1024	1024
	P. aeruginosa	> 1024	1024	> 1024	1024	1024
AcOEt	*C. albicans*	128	256	> 2048	16	64
	C. parapsilopsis	> 4096	64	> 2048	32	256
	E. coli	> 4096	512	> 2048	512	1024
	CNS	> 4096	256	> 2048	128	1024
	E. cloacae	> 4096	1024	> 2048	256	512
	K. pneumoniae	> 4096	512	> 2048	256	512
	S. aureus	> 4096	512	> 2048	512	1024
	S. epidermidis	> 4096	1024	> 2048	512	1024
	P. aeruginosa	> 4096	1024	> 2048	1024	1024
MeOH	*C. albicans*	256	512	64	256	32
	C. parapsilopsis	> 1024	64	> 1024	256	1024
	E. coli	> 1024	512	> 1024	1024	512
	CNS	> 1024	256	> 1024	256	1024
	E. cloacae	512	1024	64	1024	512
	K. pneumoniae	> 1024	256	> 1024	512	512
	S. aureus	> 1024	512	> 1024	512	256
	S. epidermidis	> 1024	1024	> 1024	1024	1024
	P. aeruginosa	> 1024	1024	64	1024	1024

extracts from stationary phase batch cultures of five marine microalgae strains (*Dunaliella* sp., *Dunaliella salina*, *Chaetoceros calcitrans*, *Chaetoceros gracilis* and *Tisochrysis lutea*) provided wide-ranging and valuable information concerning the chemical composition of these strains. As expected, extract composition was determined by the characteristics of the solvents used. In general, storage lipids were selectively extracted with hexane, whereas membrane lipids predominated in AcOEt (MGDGs) and methanol (DGDGs and SQDGs) extracts. Pigments were concentrated in the AcOEt extracts and osmolytes were the major components of methanolic extracts. Minor components such as sterols and squalene, or carbohydrates, amino acids and lactic acid were also detected in hexane and methanol extracts, respectively.

TGs were the only storage lipids produced by *Dunaliella* and *Chaetoceros* strains whereas *T. lutea* stored mainly PULCAs. The detection of brassicasterol as the only sterol in *T. lutea* and the lack of acyl chains of EPA reflected the genetic differentiation between this species and *Isochrysis galbana*.

In accordance with the classification of *Dunaliella* as a "16:3 plant", the major MGDGs identified in *Dunaliella* sp. and *D. salina* were composed by one acyl chain of ALA (C18:3) and another of DHTA (C16:4) attached to the *sn*1 and *sn*2 of the glycerol backbone, respectively. However, the two strains exhibited clear differences in the fatty acid composition of TGs. In *D. salina* there was practically no incorporation of PUFAs in TGs. β-Carotene, glycerol, derivatives of chlorophyll *a and b*, amino acids and lactic acid were found in both strains. Glycerol was the major component of the methanolic extract and also of the AcOEt extract in *D. salina*. This feature indicated a much higher production of glycerol in this strain than in *Dunaliella* sp. On the other hand, homarine that was unambiguously detected in the methanolic extract of *T. lutea* was only detected in *Dunaliella* sp. of the two *Dunaliella* strains.

C. calcitrans was characterized by high TG production. The two *Chaetoceros* strains showed the same fatty acid composition of TGs with a clear preponderance of SAFA and MUFA. EPA and ARA were detected in both TGs and MGDGs, whereas ω-4 acyl chains were only present in the glycolipid fraction. Furthermore, *Chaetoceros* strains stored, as TGs, more EPA than ARA.

The diatom (*Chaetoceros calcitrans* and *C. gracilis*) and haptophyte (*Tisochrysis lutea*) strains showed some compositional similarities. They all produced the pigments chlorophyll *a* and fucoxanthin and, in both cases, 1,4/2,5-cyclohexanetetrol (CHT) was the major polyol biosynthesized. Unlike chlorophyte strains (*Dunaliella* spp.), signals of carbohydrates were detected. For example, the two epimers of D-glucose were unambiguously identified. The results indicated, however, that glucose arose from structurally different glucans, probably chrysolaminarin in the diatoms and a highly branched (1 → 3, 1 → 6)-β-D-glucan in the haptophyte. Homarine and mannitol were only detected in *T. lutea*, but the most significant difference between *T. lutea* and *Chaetoceros* was without doubt the presence in the latter of DHSP. This compound seems to be specifically produced by diatoms, together with CHT, constituting the major component of the *Chaetoceros* methanolic extracts. In *T. lutea* methanolic extract CHT and DMSP predominated.

None of the analyzed extracts showed antibiotic activity. Promising moderate antibiofilm ability was found for the ethyl acetate extract from *C. gracilis*.

4. Experimental

4.1. Culture and extraction

The five strains used in this study were RCC5 (*Dunaliella* sp.), RCC3579 (*D. salina*), RCC1811 (*Chaetoceros calcitrans*), RCC 5953 (*C. gracilis*), and RCC1349 (*Tisochrysis lutea*) from the Roscoff Culture Collection, France (www.roscoff-culture-collection.org). Studied cultures were unialgal, non axenic transferred under laminar flow hood.

Cultures were transferred gradually from 20 mL ventiled flask (Starlab, CC7682-4825) up to 250 mL, 1L, 4L round-bottomed glass flasks. Growth media was prepare with Roscoff seawater (pH = 8.2, salinity 33‰), filtered on 0.22 µm filter (Millipore, GSWP09000) then autoclaved. Autoclaved natural seawater was added, under hood, with f/2 culture medium supplements (Guillard, 1975). Cultures were maintained at 20 °C with a light intensity of ca. 150 µE $m^{-2}s^{-1}$ provided by daylight fluorescent tubes (Philips Master TL5 H0 49W/865), with a photoperiod of 14 h light:10 h dark. Cultures were subjected to constant bubbling with sterile-filtered air. Cultures growth rate was monitored every day by flow cytometry (FACSCanto, Becton-Dickinson). After 7–14 days of growth, depending on each culture, cultures reach stationary phase. In mid-stationary phase (2 days), cultures were harvested by centrifugation (7500 rpm for 30 min) and the cell pellets were flash-frozen in liquid nitrogen, freeze-dried, then maintained at −80 °C until extraction.

Prior to extraction, freeze-dried cell pellets were first disrupted by grinding with a clean ceramic mortar to produce a fine powder. Disrupted cells were first extracted with 6 mL of hexane (3 × 2 mL in glass tubes) under ultrasound (240 W, 50 kHz) for 10 min, then centrifuged at 4600 rpm for 15 min, and the supernatant recovered in a pre-weighed 8 mL glass vial with a Teflon cap (the 3 different supernatants of about 2 mL each were pooled in this vial). The solvent was then gently evaporated in a rotavapor and the vial weighed. The residual cell pellets in the 3 tubes were kept for subsequent extraction steps. This procedure was repeated twice: first with 6 mL of AcOEt, then with 6 mL of methanol as the solvent. Prior to downstream analyses, each of the extracts was resuspended in the relevant solvent.

4.2. NMR analysis

All 1H (600 MHz) and 13C (150.9 MHz) NMR spectra were recorded on a Bruker Avance III HD 600 MHz NMR (14.0 T) spectrometer equipped with a QCI-P CryoProbe™ (proton-optimized quadruple resonance NMR 'inverse' probe). Hexane extracts were dissolved in 0.5 mL of $CDCl_3$ containing the internal standard tetramethylsilane (TMS). For the ethyl acetate and methanol extracts, the samples were prepared by dissolving the extracts in 0.5 mL of MeOD-d_4. 1H NMR

spectra of the $CDCl_3$ samples were recorded using the following parameters: relaxation delay 1 s; 90° pulse width (P1) of 6.64 μs; number of scans 128; chemical shift range 0–15 ppm. 1H NMR spectra of the MeOD-d_4 samples were recorded with solvent suppression using a gnoesy1d pulse sequence, with presaturation during relaxation delay and mixing time. The parameters were: relaxation delay 5 s; number of scans (NS) = 128; chemical shift range 0–15 ppm. 13C NMR spectra were recorded with ~12,000 scans using a relaxation delay time of 2 s, 90° pulse width of 11.7 μs, and sweep width of 0–200 ppm. Parameters for the 2D NMR spectra were as follows. For gCOSY: 2 s relaxation delay, 256 increments, 64 transients and sweep width of 10 ppm in both dimensions. A sine bell weighting function (SSB = 0) was applied prior to Fourier transformation in both dimensions (final matrix of 1024 × 1024 data points). For gHSQC–TOCSY: phase sensitive via echo-antiecho mode, 2 s relaxation delay, 256 increments, 64 transients, a mixing time of 80 ms, and a sweep width of 12 and 200 ppm for the 1H and 13C dimensions, respectively. A squared cosine weighting function (SSB = 2) was applied prior to Fourier transformation in both dimensions (1024 × 1024 data points). For multiplicity edited gHSQC: phase sensitive mode using the echo-antiecho technique, 1.5 s relaxation delay, 256 increments, 64 transients and a sweep width of 12 and 200 ppm for the 1H and 13C dimensions, respectively. Spectra were processed using a squared cosine weighting function (SSB = 2) prior to Fourier transformation in both dimensions (1024 × 1024 data points). For gHMBC: magnitude mode, 2 s relaxation delay, 128 increments, 128 transients and a sweep width of 12 and 200 ppm for the 1H and 13C dimensions, respectively. Spectra were processed using a sine bell weighting function (SSB = 0) prior to Fourier transformation in both dimensions (2048 × 1024 data points). For z-COSY: phase sensitive using the States-TPPI technique, 2 s relaxation delay, 256 increments, 64 transients and a sweep width of 10 ppm in both dimensions. Spectra were processed using a squared cosine weighting function (SSB = 2) prior to Fourier transformation in both dimensions (1024 × 1024 data points). Standard Bruker software (TopSpin 3.6) was used for the acquisition and processing of NMR spectra.

Integration of selected resonances was performed using the deconvolution algorithm present in MNova 10.1 software after removal of residual solvent signal and normalization to the total spectral area. Deconvoluted signals for specific metabolites were then divided by the number of hydrogen in order to obtain its relative molar content (mol %).

4.3. Bioactivity assays

Antibiotic assays were performed against a Gram-positive bacterium (*Staphylococcus aureus*), a Gram-negative bacterium (*Escherichia coli*) and a fungus (*Candida parapsilosis*). The three pathogens were inoculated in 5 mL Mueller-Hinton medium from glycerol stocks, and incubated overnight at 37 °C with agitation at 250 rpm. After OD_{600} spectrophometric assessment, 5×10^5 cfu/mL of each pathogen were used for each antibiotic assay.

A mixture of 5:95 DMSO:H_2O was added to each dry microalgal extract, and the vial was sonicated until total resuspension. Serial two-fold dilutions of the resuspended extract were carried out in a microtitre plate (one row per extract) with 50 μL of sterile Milli-Q water pre-added to all wells. The RCC5 tested dilutions ranges were between 14.4 and 0.9 mg/mL (for hexane), 9.45 to 0.59 mg/mL for ethyl acetate and 8.85 to 0.55 mg/mL for methanol. The RCC1811 tested dilutions ranges were between 12.85 and 0.8 mg/mL (for hexane), 2.7 to 0.17 mg/mL (for ethyl acetate) and 4.55 to 0.28 mg/mL (for methanol). The RCC3579 tested dilutions ranges were between 26.5 and 1.65 mg/mL (for hexane), 6.55 to 0.4 mg/mL (for ethyl acetate) and 19.98 to 1.24 mg/mL (for methanol). The RCC5953 tested dilutions ranges were between 33 and 0.2 mg/mL (for hexane), 8.85 to 0.55 mg/mL (for ethyl acetate) and 17.02 to 1.06 mg/mL (for methanol). The RCC1349 tested dilutions ranges were between 8.65 and 0.54 mg/mL (for hexane), 3.05 to 0.19 mg/mL (for ethyl acetate) and 17.75 to 1.11 mg/mL (for methanol). 50 μL of the corresponding microorganism suspension (5×10^5 cfu/mL) in Mueller-Hinton 2x, were added to all wells in the microtitre row. Negative controls (wells without microorganism) and positive controls (wells without extract) were also included.

Microdilution plates for antibiotic assays were incubated overnight at 37 °C and then all wells were replicated to fresh solid medium: MSA (mannitol salt agar) for *S. aureus*, EMB (eosin methylene blue) for *E. coli,* and Sabouraud agar for *C. parapsilosis.* Bacteriostatic/fungistatic activities (growth inhibition in microdilution but normal growth in replicated plate) and bactericidal/fungicidal activities (absence of growth in both microdilution and replicated plates) are detected with this method.

Biofilm inhibition of these extracts was assayed using *E. coli, Klebsiella pneumoniae, Enterobacter cloacae, Pseudomonas aeruginosa, S. aureus, Coagulase-negative Streptococcus, S. epidermidis, C. albicans* and *C. parapsilosis*. The bacteria were cultured overnight at 37 °C (30 °C in the case of *E. coli*) in TSB culture medium (Gram-positive bacteria); M63 (*E. coli*); LB (the remaining Gram-negative bacteria); or Yeast Nitrogen Base (*Candida* sp.). 50 μL of the relevant culture medium were added to each well of the microtitre plate. 50 μL of the microalgae extract in a known concentration was added to the first well (at four times the concentration to be evaluated, e.g. to evaluate the minimal inhibitory concentration, MIC, in a range of 4-0.125 mg/mL, an initial concentration of 16 mg/mL must be prepared). After mixing, 50 μL were transferred into the next well and so on, resulting in serial dilutions.

For each strain grown overnight, a 0.5 McFarland inoculum was prepared (using a nephelometer) and diluted in Falcon tubes containing 10 mL of the appropriate culture medium (1 tube per strain). 50 μL of bacterial inoculum were added to all of the microtitre wells, except the well used as a negative control. In each experiment, a positive control (culture medium plus bacteria) and a negative control (only culture medium) were used. Ten dilutions of each extract were assayed. The concentrations ranged from 4096 mg/L to 8 mg/L or from 1024 mg/L to 2 mg/L depending of the initial amount of the extract.

The plate was covered with an adhesive foil and Parafilm and incubated at 37 °C (30 °C for *E. coli*) for 48 h. Following the incubation period, the supernatant was discarded and the wells gently washed 1 to 2 times with 1% PBS. The biofilm was fixed for approximately 20 min at 60 °C to evaporate all of the PBS in each well. 200 μL of 2% violet crystal (VC) were added to each well and incubated for 10 min at room temperature. The VC was discarded and wells were washed 1 to 2 times with 1% PBS. The stained biofilm was then completely dried for 40 min at 60 °C. Finally, 200 μL of 33% acetic acid were added to each well to resuspend the biofilm. The absorbance was read at 580 λ in a spectrophotometer always discounting the value obtained in the negative control.

Minimal biofilm inhibitory concentration (MBIC) was defined as the lowest extract concentration that inhibited biofilm formation.

Acknowledgements

Funding from the European Union's Horizon 2020 research and innovation program under grant agreement no. 634588 (NOMORFILM) is gratefully acknowledged.

Appendix A. Supplementary data

Supplementary data to this article can be found online at https://doi.org/10.1016/j.phytochem.2019.05.001.

References

Abd El-Baky, H.H., El Baz, F.K., El-Baroty, G.S., 2004. Production of lipids rich in omega 3 fatty acids from the halotolerant alga *Dunaliella salina.* Biotech 3, 102–108.

Abraham, R.J., Rowan, A.E., 1991. Nuclear magnetic resonance spectroscopy of Chlorophyll. In: Scheer, Hugo (Ed.), Chlorophylls. CRC Press, Boca Raton u.a, pp. 797–834.

Affeld, S., Wägele, H., Avila, C., Kehraus, S., Köning, G.M., 2006. Distribution of homarine in some opisthobranchia (gastropoda: Mollusca) bonn. Zool. Beitr. 55, 181–190.

Akhter, M., Majumdar, R.D., Firtier-McGill, B., Soong, R., Liagati-Mobarhan, Y., Simpson, M., Arhomditsis, G., Scmidt, S., Heumann, H., Simpson, A.J., 2016. Identification of aquatically available carbon from algae through solution-state NMR of whole 13C-labelled cells. Anal. Bional. Chem. 408, 4357–4370.

Azizan, A., Ahamad Bustamam, M.S., Maulidiani, M., Shaari, K., Ismail, I.S., Nagao, N., Abas, F., 2018. Metabolite profiling of the microalgal diatom *Chaetoceros calcitrans* and correlation with antioxidant and nitric oxide inhibitory activities via 1H NMR-based metabolomics. Mar. Drugs 16, 154. https://doi.org/10.3390/md16050154.

Beal, C.M., Webber, M.E., Ruoff, R.S., Hebner, R.E., 2010. Lipid analysis of *Neochloris oleoabundans* by liquid state NMR. Biotechnol. Bioeng. 106, 573–583.

Ben-Amotz, A., Avron, M., 1973. The role of glycerol in the osmotic regulation of the halophilic alga *Dunaliella parva*. Plant Physiol. 51, 875–878.

Bendif, El M., Probert, I., Schoreder, D.C., de Vargas, C., 2013. On the description of *Tisochrysis lutea* gen. nov. sp. nov. and *Isochrysis nuda* sp. nov. in the Isochrysidales, and the transfer of Dicrateria to the Prymnesiales (Haptophyta). J. Appl. Phycol. 25, 1763–1776.

Bhattacharjee, M., 2016. Pharmaceutically valuable bioactive compounds of algae. Asian J. Pharmaceut. Clin. Res. 9, 43–47.

Blunt, J.W., Copp, B.R., Keyzers, R.A., Munro, M.H.G., Prinsep, M.R., 2015. Marine natural products. Nat. Prod. Rep. 32, 116–211.

Borchman, D., Yappert, M.C., Milliner, S.E., Smith, R.J., Bhola, R., 2013. Confirmation of the presence of squalene in human eyelid lipid by heteronuclear single quantum correlation spectroscopy. Lipids 48, 1269–1277.

Brown, M.R., 1991. The amino-acid and sugar composition of 16 species of microalgae used in marineculture. J. Exp. Mar. Biol. Ecol. 145, 79–99.

Busby, W.F., 1966. Sulfopropanedial and cysteinolic acid in the diatom. Biochim. Biophys. Acta 121, 160–161.

Chauton, M.S., Størseth, T.R., 2018. HR-MAS NMR spectroscopy of marine microalgae. In: Webb, G.A. (Ed.), Modern Magnetic Resonance, second ed. Springer, Dordrecht, pp. 1927–1935.

Chia, S.R., Chew, K.W., Show, K.W., Yap, Y.J., Ong, H.C., Ling, T.C., Chang, J.S., 2018. Analysis of economic and environmental aspects of microalgae biorefinery for biofuels production: a review. Biotechnol. J. https://doi.org/10.1002/biot.201700618.

Da Costa, F., Petton, B., Mingant, C., Bourgaran, G., Rouxel, C., Quéré, C., Wikfors, G.H., Soudnat, P., Robert, R., 2016. Influence of one selected *Tisochrysis lutea* strain rich in lipids on *Crassostrea gigas* larval development and biochemical composition. Aquacult. Nutr. 22, 813–836.

Dais, P., Misiak, M., Hatzakis, E., 2015. Analysis of marine dietary supplements using NMR spectroscopy. Anal. Methods 7, 5226–5238.

Deborde, C., Moing, A., Roch, L., Jacob, D., Rolin, D., Giraudeau, P., 2017. Plant metabolism as studied by NMR spectroscopy. Prog. Nucl. Magn. Reson. Spectrosc. 102–103, 61–97.

Desbois, A.P., Mearns-Spragg, A., 2009. A fatty acid from the diatom Phaeodactylum tricornutum is antibacterial against diverse bacteria including multi-resistant *Staphylococcus aureus* (MRSA). Mar. Biotechnol. 11, 45–52.

Diehl, B.W.K., Heling, H., Riedl, I., Heinz, E., 1995. 13C-NMR analysis of the positional distribution of fatty acids in plant glycolipids. Chem. Phys. Lipids 77, 147–153.

Dobretsov, S., Teplitski, M., Alagely, A., Gunasekera, S.P., Paul, V.J., 2010. Malyngolide from the cyanobacterium *Lyngbya majuscula* interferes with quorum sensing circuitry. Environ. Microbiol. Rep. 2, 739–744.

Dunstan, G.A., Volkman, J.K., Barrett, S.M., Leroi, J.M., Jeffrey, S.W., 1994. Essential polyunsaturated fatty acids from 14 species of diatom (Bacillariophyceae). Phytochemistry 35, 155–161.

Durham, B.P., Sharma, S., Luo, H., Smith, C.B., Amin, S.A., Bender, S.J., Dearth, S.P., Van Mooy, B.A.S., Campagna, S.R., Kujawinski, E.B., Armbrust, E.V., Moran, M.A., 2015. Cryptic carbon and sulfur cycling between surface ocean plankton. Proc. Natl. Acad. Sci. Unit. States Am. 112, 453–457.

Eltgroth, M.L., Watwood, R.L., Wolfe, G.V., 2005. Production and cellular localization of neutral long-chain lipids in the haptophyte algae *Isochrysis galbana* and *Emiliania huxleyi*. J. Phycol. 41, 1000–1009.

Englert, G., Bjørnland, T., Liaaen-Jensen, S., 1990. 1D and 2D NMR study of some allenic carotenoids of the fucoxanthin series. Magn. Reson. Chem. 28, 519–528.

Fan, T.W.M., Lane, A.N., 2016. Applications of NMR spectroscopy to systems biochemistry. Prog. Nucl. Magn. Reson. Spectrosc. 92–93, 18–53.

Ford, C.W., Percival, E., 1965. The Carbohydrates of *Phaeodactylum tricornutum*. Part I. Preliminary examination of the organism, and characterisation of low molecular weight material and of a glucan. J. Chem. Soc. 7035–7041.

Fujii, S., Nishimoto, N., Notoya, A., Hellebust, J.A., 1995. Growth and osmoregulation of *Chaetoceros muelleri* (Bacillariophyceae) in relation to salinity. Plant Cell Physiol. 36, 759–764.

Garnier, M., Bougaran, G., Pavlovic, M., Berard, J.B., Carrier, G., Charrier, A., Le Grand, F., Lukomska, E., Rouxel, C., Schreiber, N., Cadoret, J.P., Rogniaux, H., Saint-Jean, B., 2016. Use of a lipid rich strain reveals mechanisms of nitrogen limitation and carbon partitioning in the haptophyte *Tisochrysis lutea*. Algal Res 20, 229–248.

Garza-Sánchez, F., Chapman, D.J., Cooper, J.B., 2009. *Nitzschia ovalis* (Bacillariophyceae) mono lake strain accumulates 1,4/2,5 cyclohexanetetrol in response to increased salinity. J. Phycol. 45, 395–403.

Gebser, B., Pohnert, G., 2013. Synchronized regulation of different zwitterionic metabolites in the osmoadaption of phytoplankton. Mar. Drugs 11, 2168–2182.

Granum, E., Myklestad, S.M., 2001. Mobilization of β-1,3-glucan and biosynthesis of amino acids induced by NH_4^+ addition to N-limited cells of the marine diatom *Skeletonema costatum* (Bacillariophyceae). J. Phycol. 37, 772–782.

Guillard, R.R.L., 1975. Culture of phytoplankton for feeding marine invertebrates. In: Smith, W.L., Chanley, M.H. (Eds.), Culture of Marine Invertebrate Animals. Springer, Boston, MA, pp. 29–60.

Guiry, M.D., 2012. How many species of algae are there? J. Phycol. 48, 1057–1063.

Gunstone, F.D., Seth, S., 1994. A study of the distribution of eicosapentaenoic acid and docosahexaenoic acid between the α and β glycerol chains in fish oils by 13C-NMR spectroscopy. Chem. Phys. Lipids 72, 119–126.

Gunstone, F.D., 1990. 13C-NMR spectra of some synthetic glycerol esters alone and as mixtures. Chem. Phys. Lipids 56, 195–199.

Gupta, V., Thakur, R.S., Reddy, C.R.K., Jha, B., 2013. Central metabolic processes of marine macrophytic algae revealed from NMR based metabolome analysis. RSC Adv. 3, 7037–7047.

Herrero, M., Ibáñez, E., Cifuentes, A., Reglero, G., Santoyo, S., 2006. *Dunaliella salina* microalga pressurized liquid extracts as potential antimicrobials. J. Food Prot. 69, 2471–2477.

Jaspars, M., De Pascale, D., Andersen, J.H., Reyes, F., Crawfrod, A.D., Ianora, A., 2016. The marine biodiscovery pipeline and ocean medicines of tomorrow. J. Mar. Biol. Assoc. U. K. 96, 151–158.

Keller, M.D., Kiene, R.P., Matrai, P.A., Bellows, W.K., 1999. Production of glycine betaine and dimethylsulfoniopropionate in marine phytoplankton. II. N-limited chemostat cultures. Mar. Biol. 135, 237–248.

Kiene, R.P., Linn, L.J., Bruton, J.A., 2000. New and important roles for DMSP in marine microbial communities. J. Sea Res. 43, 209–224.

Kim, S.W., Ban, S.H., Ahn, C.Y., Oh, H.M., Chung, H., Cho, S.H., Park, Y.M., Liu, J.R., 2006. Taxonomic discrimination of cyanobacteria by metabolic fingerprinting using proton nuclear magnetic resonance spectra and multivariate statistical analysis. J. Plant Biol. 49, 271–275.

Kim, S.H., Ahn, H.M., Lim, S.R., Hong, S.J., Cho, B.K., Lee, H., Lee, C.G., Choi, H.K., 2015. Comparative lipidomic profiling of two *Dunaliella tertiolecta* strains with different growth temperatures under nitrate-deficient conditions. J. Agric. Food Chem. 63, 880–887.

Kobayashi, Y., Torii, A., Kato, M., Adachi, K., 2007. Accumulation of cyclitols functioning as compatible solutes in the haptophyte alga *Pavlova* sp. Phycol. Res. 55, 81–90.

Kuczynska, P., Jemiola-Rzeminska, M., Stralka, K., 2015. Photosynthetic pigments in diatoms. Mar. Drugs 13, 5847–5881.

Kumar, R., Bansal, V., Patel, M.B., Sarpal, A.S., 2014. Compositional analysis of algal biomass in a Nuclear Magnetic Resonance (NMR) tube. J. Algal Biomass Utln. 5, 36–45.

Lang, I., Hodac, L., Froedl, T., Feussner, I., 2011. Fatty acid profiles and their distribution patterns in microalgae: a comprehensive analysis of more than 2000 strains from the SAG culture collection. BMC Plant Biol. 11, 124/1–124/16.

Lauritano, C., Andersen, J.H., Hansen, E., Albrigtsen, M., Escalera, L., Esposito, F., Helland, K., Hanssen, K.Ø., Romano, G., Ianora, A., 2016. Bioactivity screening of microalgae for antioxidant, anti-inflammatory, anticancer, anti-diabetes, and antibacterial activities. Frot. Mar. Sci. 3, 68/1–68/12.

LewisOscar, F., Nithya, C., Bakkiyaraj, D., Arunkumar, M., Alharbi, N.S., Thajuddin, N., 2017. Biofilm inhibitory effect of *Spirulina platensis* extracts on bacteria of clinical significance. Proc. Natl. Acad. Sci. India B Biol. Sci. 87, 537–544.

Liu, C.P., Lin, L.P., 2001. Ultrastructural study and lipid formation of *Isochrysis* sp. CCMP1324. Bot. Bull. Acad. Sin. (Taipei) 42, 207–214.

Logvinov, S., Gerasimenko, N., Esipov, A., Denisenko, V.A., 2015. Examination of the structures of several glycerolipids from marine macroalgae by NMR and GC-MS. J. Phycol. 51, 1066–1074.

Maras, A., Erden, M., Seçen, H., Sütbeyaz, Y., 1998. One-pot synthesis from 1,4-cyclohexadiene of (±)-1,4/2,5-cyclohexanetetrol, a naturally occurring cyclitol derivative. Carbohydr. Res. 308, 435–437.

Marlowe, I.T., Brassell, S.C., Eglinton, G., Green, J.C., 1984. Long chain unsaturated ketones and esters in living algae and marine sediments. Org. Geochem. 6, 135–141.

Matos, Â.P., 2017. The impact of microalgae in food science and technology. J. Am. Oil Chem. Soc. 94, 1333–1350.

Mayer, A.M.S., Rodríguez, A.D., Taglialatela-Scafati, O., Fusetani, N., 2013. Marine pharmacology in 2009-2011: marine compounds with antibacterial, antidiabetic, antifungal, anti-inflammatory, antiprotozoal, antituberculosis, and antiviral activities; affecting the immune and nervous systems, and other miscellaneous mechanisms of action. Mar. Drugs 11, 2510–2573.

Mendiola, J.A., Torres, C.F., Toré, A., Martín-Álvarez, P.J., Santoyo, S., Arredondo, B.O., Señoráns, F.J., Cifuentes, A., Ibáñez, E., 2007. Use of supercritical CO_2 to obtain extracts with antimicrobial activity from *Chaetoceros muelleri* microalga. A correlation with their lipidic content. Eur. Food Res. Technol. 224, 505–510.

Mendiola, J.A., Santoyo, S., Cifuentes, A., Reglero, G., Ibáñez, E., Señoráns, F.J.J., 2008. Antimicrobial activity of sub- and supercritical CO_2 extracts of the green alga *Dunaliella salina*. Food Prot 71, 2138–2143.

Millar, A.A., Smith, M.A., Kunst, L., 2000. All fatty acids are not equal: discrimination in plant membrane lipids. Trends Plant Sci. 5, 95–101.

Miller, M.R., Quek, S.-Y., Staeher, K., Nalder, T., Packer, M.A., 2014. Changes in oil content, lipid class and fatty acid composition of the microalga *Chaetoceros calcitrans* over different phases of batch culture. Aquacult. Res. 45, 1634–1647.

Mobin, S., Alam, F., 2017. Some promising microalgal species for commercial applications: a review. Energy Procedia 110, 510–517.

Mulders, K.J.M., Weesepoel, Y., Lamers, P.P., Vincken, J.P., Martens, D.E., Wijffels, R.H., 2013. Growth and pigment accumulation in nutrient-depleted *Isochrysis* aff. *galbana* T-ISO. J. Appl. Phycol. 25, 1421–1430.

Nieva-Echevarría, B., Goicoechea, E., Manzanos, M.J., Guillén, M.D., 2014. A method based on 1H NMR spectral data useful to evaluate the hydrolysis level in complex lipid mixtures. Food Res. Int. 66, 379–387.

Nuzzo, G., Gallo, C., d'Ippolito, G., Cutignano, A., Sardo, A., Fontana, A., 2013. Composition and quantitation of microalgal lipids by ERETIC 1H NMR method. Mar. Drugs 11, 3742–3753.
O'Neil, G.W., Knothe, G., Williams, J.R., Burlow, N.P., Culler, A.R., Corliss, J.M., Carmichel, C.A., Reddy, C.M., 2014. Synthesis and analysis of an alkenone-free biodiesel from *Isochrysis* sp. Energy Fuels 28 2877-2683.
Obando, C.Z., Linossier, I., Kervarek, N., Zubia, M., Turquet, J., Faÿ, F., Rehel, K., 2016. Rapid identification of osmolytes in tropical microalgae and cyanobacteria by 1H HR-MAS NMR spectroscopy. Talanta 153, 372–380.
Obata, T., Schoenefeld, S., Kranhnert, I., Bergmann, S., Scheffek, A., Ferni, A.R., 2013. Gas-Chromatography Mass-Spectrometry (GC-MS) based metabolite profiling reveals mannitol as a major storage carbohydrate in the coccolithophorid alga *Emiliania huxleyi*. Metabolites 3, 168–184.
Ohta, S., Shiomi, Y., Kawahima, A., Aozasa, O., Nakao, T., Nagate, T., Kitamura, K., Miyata, H., 1995. Antibiotic effect of linolenic acid from *Chlorococcum* strain HS-101 and *Dunaliella primolecta* on methicillin-resistant *Staphylococcus aureus*. J. Appl. Phycol. 7 212-127.
Patterson, G.W., Tsittsa-Tsardis, E., Wikfors, G.H., Galdu, P.K., Chitwood, D.J., Harrison, D., 1994. Sterols and alkenones of *Isochrysis*. Phytochemistry 35, 1233–1236.
Peng, J., Yuan, J.P., Wu, C.F., Wang, J.H., 2011. Fucoxanthin, a marine carotenoid present in brown seaweeds and diatoms: metabolism and bioactivities relevant to human health. Mar. Drugs 9, 1806–1828.
Pollesello, P., Toffanin, R., Murano, E., Paoletti, S., Rizzo, R., Kvam, B.J., 1992. Lipid extracts from different algal species: 1H and13C-NMR spectroscopic studies as a new tool to screen differences in the composition of fatty acids, sterols and carotenoids. J. Appl. Phycol. 4, 315–322.
Rechka, J.A., Maxwell, J.R., 1987. Unusual long chain ketones of algal origin. Adv. Org. Geochem. 13, 727–734.
Réveillon, D., Tunin-Ley, A., Grondin, I., Othmani, A., Zubia, M., Bunet, R., Turquet, J., Culioli, G., Briand, J.F., 2018. Exploring the chemodiversity of tropical microalgae for the Discovery of natural antifouling compounds. J. Appl. Phycol. https://doi.org/10.1007/s10811-018-1594-z.
Roleda, M.Y., Slocombe, S.P., Leakey, R.J.G., Day, J.G., Bell, E.M., Stanley, M.S., 2013. Effects of temperature and nutrient regimes on biomass and lipid production by six oleaginous microalgae in batch culture employing a two-phase cultivation strategy. Bioresour. Technol. 129, 439–449.
Romano, G., Costantini, M., Sansone, C., Lauritano, C., Ruocco, N., Ianora, A., 2017. Marine microorganisms as a promising and sustainable source of bioactive molecules. Mar. Environ. Res. 128, 58–69.
Romero, M., Diggle, S.P., Heeb, S., Cámara, M., Otero, A., 2008. Quorum quenching activity in *Anabaena* sp. PCC7120: identification of AiiC, a novelAHL-acylase. FEMS Microbiol. Lett. 280, 73–80.
Roy, A.B., Hewlins, M.J.E., Ellis, A.J., Harwood, A.J., White, G.F., 2003. Glycolytic breakdown of sulfoquinovose in bacteria: a missing link in the sulfur cycle. Appl. Environ. Microbiol. 69, 6434–6441.
Ruffell, S.E., Müller, K.M., McConkey, B.J., 2016. Comparative assessment of microalgal fatty acids as topical antibiotics. J. Appl. Phycol. 28, 1695–1704.
Sacchi, R., Medina, I., Aubourg, S.P., Giuducuanni, I., Paolillo, L., Addeo, F., 1993. Quantitative high-resolution 13C NMR analysis of lipids extracted from the white muscle of Atlantic tuna (*Thunnus alalunga*). J. Agric. Food Chem. 41, 1247–1253.
Sacchi, R., Addeo, F., Paolillo, L., 1997. 1H and 13C NMR of virgin olive oil. An overview. Magn. Reson. Chem. 35, S133–S145.
Sadovskaya, I., Souissi, A., Souissi, S., Grard, T., Lencel, P., Greene, C.M., Duin, S., Dmitrenok, P.S., Chizhov, A.O., Shaskov, A.S., Usov, A.I., 2014. Chemical structure and biological activity of a highly branched (1 → 3,1 → 6)-β-d-glucan from *Isochrysis galbana*. Carbohydr. Polym. 111, 139–148.
Saha, M., Rempt, M., Grosser, K., Pohnert, G., Werinberger, F., 2011. Surface-associated fucoxanthin mediates settlement of bacterial epiphytes on the rockweed *Fucus vesiculosus*. Biofouling 27, 423–433.
Sakano, Y., Mutsuga, M., Tanaka, R., Suganuma, H., Inakuma, T., Toyoda, M., Goda, Y., Shibuya, M., Ebizuka, Y., 2005. Inhibition of human lanosterol synthase by the constituents of *Colocasia esculenta* (Taro). Biol. Pharm. Bull. 28, 299–304.
Salinero, C., Feás, X., Mansilla, J.P., Seijas, J.A., Vázquez-Tato, M.P., Vela, P., Sainz, M.J., 2012. 1H-nuclear magnetic resonance analysis of the triacylglyceride composition of cold-pressed oil from *Camellia japonica*. Molecules 17, 6716–6727.
Sarker, S.D., Latif, Z., Gray, A.I., 2006. Natural Products Isolation, second ed. Humana Press, New Jersey.
Sarpal, A.S., Teixeira, C.M.L.L., Silva, P.R.M., Lima, G.M., Silva, S.R., Monteiro, T.V., Cunha, V.S., Daroda, R.J., 2015. Determination of lipid content of oleaginous microalgal biomass by NMR spectroscopic and GC–MS techniques. Anal. Bioanal. Chem. 407, 3799–3816.
Sarpal, A.S., Teixeira, C.M.L.L., Silva1, P.R.M., da Costa Monteiro, T.V., da Silva1, J.I., da Cunha, V.S., Daroda, R.J., 2016a. NMR techniques for determination of lipid content in microalgal biomass and their use in monitoring the cultivation with biodiesel potential. Appl. Microbiol. Biotechnol. 100, 2471–2485.
Sarpal, A.S., Sharma, B.K., Scott, J., Kumar, R., Sugmaran, V., Chopra, A., Bansal, V., Rajagopalan, N.K., 2016b. Compositional analyses of oil extracts of microalgae biomasses by NMR and chromatographic techniques. J. Anal. Bioanal. Sep. Tech. 1, 17–41.
Sarpal, A.S., Costa, I.C.R., Teixeira, C.M.L.L., Filocomo, D., Candido, R., Silva, P.R.M., Cunha, V.S., Daroda, R.J., 2016c. Investigation of biodiesel potential of biomasses of microalgaes chlorella, Spirulina and Tetraselmis by NMR and GC-MS techniques. J. Biotechnol. Biomater. 6, 1000220/1–000220/15.
Satyarthi, J.K., Srinivas, D., Ratnasamy, P., 2009. Estimation of free fatty acid content in oils, fats, and biodiesel by 1H NMR spectroscopy. Energy Fuels 23, 2273–2277.
Serive, B., Nicolau, E., Bérard, J.B., Kaas, R., Pasquet, V., Picot, L., Cadoret, J.P., 2017. Community analysis of pigment patterns from 37 microalgae strains reveals new carotenoids and porphyrins characteristic of distinct strains and taxonomic groups. PLoS One 12, e0171872/1–e0171872/35.
Shannon, E., Abu-Ghannam, N., 2016. Antibacterial derivatives of marine algae: an overview of pharmacological mechanisms and applications. Mar. Drugs 14, 81/1–81/23.
Slattery, M., Hamann, M.T., McClintock, J.B., Perry, T.L., Puglisi, M.P., Yoshida, W.Y., 1997. Ecological roles for water-borne metabolites from Antarctic soft corals. Mar. Ecol. Prog. Ser. 161, 133–144.
Sobolev, A.P., Brosio, E., Gianferri, R., Segre, A.L., 2005. Metabolic profile of lettuce leaves by high-field NMR spectra. Magn. Reson. Chem. 43, 625–638.
Størseth, T.R., Hansen, K., Skjermo, J., Krane, J., 2004. Characterization of a β-d-(1 → 3)-glucan from the marine diatom *Chaetoceros müilleri* by high-resolution magic-angle spinning NMR spectroscopy on whole algal cells. Carbohydr. Res. 339, 421–424.
Størseth, T.R., Kirkvold, S., Skjermo, J., Reitan, K.I., 2006. A branched β-d-(1→3,1→6)-glucan from the marine diatom *Chaetoceros debilis* (Bacillariophyceae) characterized by NMR. Carbohydr. Res. 341, 2108–2114.
Sun, Y., Lin, Y., Cao, X., Xiang, L., Qi, J., 2014. Sterols from *Mytilidae* show anti-aging and neuroprotective effects via anti-oxidative activity. Int. J. Mol. Sci. 15, 21660–21673.
Thompson Jr., G.A., 1996. Lipids and membrane function in green algae. Biochem. Bioph. Acta 1302, 17–45.
Thormar, E., 2011. Lipids and Essential Oils as Antimicrobial Agents. John Wiley & Sons, Chichester.
Tsuji, Y., Yamazaki, M., Suzuki, I., Shiraiwa, Y., 2015. Quantitative analysis of carbon flow into photosynthetic products functioning as carbon storage in the marine coccolithophore. *Emiliania huxleyi*. Mar. Biotechnol. 17, 428–440.
Tsukida, K., Saiki, K., Sugira, M., 1981. Structural elucidation of the main *cis*-β-carotenes. J. Nutr. Sci. Vitaminol. 27, 551–561.
Vidal, N.P., Manzanos, M.J., Goicoechea, E., Guillén, M.D., 2012. Quality of farmed and wild sea bass lipids studied by 1H NMR: usefulness of this technique for differentiation on a qualitative and a quantitative basis. Food Chem. 135, 1583–1591.
Viso, A.C., Marty, J.C., 1993. Fatty acids from 28 marine microalgae. Phytochemistry 34, 1521–1533.
Volkman, J.K., Egliton, G., Corner, E.D.S., Forseberg, T.E.V., 1980. Long-chain alkenes and alkenones in the marine coccolithophorid *Emiliania huxleyi*. Phytochemistry 19, 2619–2622.
Volkman, J.K., Jeffrey, S.W., Nichols, P.D., Rogers, G.I., Garland, C.D., 1989. Fatty acid and lipid composition of 10 species of microalgae used in mariculture. J. Exp. Mar. Biol. Ecol. 128, 219–240.
Weete, J.D., Kulifaj, M., Montant, C., Nes, W.R., Sancholle, M., 1985. Distribution of sterols in fungi. II. Brassicasterol in Tuber and Terfezia species. Can. J. Microbiol. 31, 1127–1130.
Wikfors, G.H., Ohno, M., 2001. Impact of algal research in aquaculture. J. Phycol. 37, 968–974.
Yancey, P.H., 2005. Organic osmolytes as compatible, metabolic and counteracting cytoprotectants in high osmolarity and other stresses. J. Exp. Biol. 208, 2819–2830.
Yao, L., Gerde, J.A., Lee, S.L., Wang, T., Harrata, K.A., 2015. Microalgae lipid characterization. J. Agric. Food Chem. 63, 1773–1787.
Zheng, C.J., Yoo, H.Y., Kim, Y.H., Kim, W.G., 2005. Fatty acid synthesis is a target for antibacterial activity of unsaturated fatty acids. FEBS Lett. 579, 5157–5162.
Zhukova, N.V., Aizdaicher, N.A., 1995. Fatty acid composition of 15 species of marine microalgae. Phytochemistry 39, 351–356.